University Transportation Research Center - Region 2

Final Report

A Probability-Based Approach for Assessment of Roadway Safety Hardware

Performing Organization: Manhattan College
University of North Carolina at Charlotte

March 2017

Sponsor:
University Transportation Research Center - Region 2

University Transportation Research Center - Region 2

The Region 2 University Transportation Research Center (UTRC) is one of ten original University Transportation Centers established in 1987 by the U.S. Congress. These Centers were established with the recognition that transportation plays a key role in the nation's economy and the quality of life of its citizens. University faculty members provide a critical link in resolving our national and regional transportation problems while training the professionals who address our transportation systems and their customers on a daily basis.

The UTRC was established in order to support research, education and the transfer of technology in the field of transportation. The theme of the Center is "Planning and Managing Regional Transportation Systems in a Changing World." Presently, under the direction of Dr. Camille Kamga, the UTRC represents USDOT Region II, including New York, New Jersey, Puerto Rico and the U.S. Virgin Islands. Functioning as a consortium of twelve major Universities throughout the region, UTRC is located at the CUNY Institute for Transportation Systems at The City College of New York, the lead institution of the consortium. The Center, through its consortium, an Agency-Industry Council and its Director and Staff, supports research, education, and technology transfer under its theme. UTRC's three main goals are:

Research

The research program objectives are (1) to develop a theme based transportation research program that is responsive to the needs of regional transportation organizations and stakeholders, and (2) to conduct that program in cooperation with the partners. The program includes both studies that are identified with research partners of projects targeted to the theme, and targeted, short-term projects. The program develops competitive proposals, which are evaluated to insure the mostresponsive UTRC team conducts the work. The research program is responsive to the UTRC theme: "Planning and Managing Regional Transportation Systems in a Changing World." The complex transportation system of transit and infrastructure, and the rapidly changing environment impacts the nation's largest city and metropolitan area. The New York/New Jersey Metropolitan has over 19 million people, 600,000 businesses and 9 million workers. The Region's intermodal and multimodal systems must serve all customers and stakeholders within the region and globally.Under the current grant, the new research projects and the ongoing research projects concentrate the program efforts on the categories of Transportation Systems Performance and Information Infrastructure to provide needed services to the New Jersey Department of Transportation, New York City Department of Transportation, New York Metropolitan Transportation Council , New York State Department of Transportation, and the New York State Energy and Research Development Authorityand others, all while enhancing the center's theme.

Education and Workforce Development

The modern professional must combine the technical skills of engineering and planning with knowledge of economics, environmental science, management, finance, and law as well as negotiation skills, psychology and sociology. And, she/he must be computer literate, wired to the web, and knowledgeable about advances in information technology. UTRC's education and training efforts provide a multidisciplinary program of course work and experiential learning to train students and provide advanced training or retraining of practitioners to plan and manage regional transportation systems. UTRC must meet the need to educate the undergraduate and graduate student with a foundation of transportation fundamentals that allows for solving complex problems in a world much more dynamic than even a decade ago. Simultaneously, the demand for continuing education is growing – either because of professional license requirements or because the workplace demands it – and provides the opportunity to combine State of Practice education with tailored ways of delivering content.

Technology Transfer

UTRC's Technology Transfer Program goes beyond what might be considered "traditional" technology transfer activities. Its main objectives are (1) to increase the awareness and level of information concerning transportation issues facing Region 2; (2) to improve the knowledge base and approach to problem solving of the region's transportation workforce, from those operating the systems to those at the most senior level of managing the system; and by doing so, to improve the overall professional capability of the transportation workforce; (3) to stimulate discussion and debate concerning the integration of new technologies into our culture, our work and our transportation systems; (4) to provide the more traditional but extremely important job of disseminating research and project reports, studies, analysis and use of tools to the education, research and practicing community both nationally and internationally; and (5) to provide unbiased information and testimony to decision-makers concerning regional transportation issues consistent with the UTRC theme.

Project No(s):
UTRC/RF Grant No: 49198-11-27

Project Date: March 2017

Project Title: A Probability-Based Approach for Assessment of Roadway Safety Hardware

Project's Website:
http://www.utrc2.org/research/projects/probability-based-assessment

Principal Investigator(s):
Qian Wang
Assistant Professor
Dept. of Civil and Environmental Engineering
Manhattan College
Bronx, NY 10471
Tel: (718) 862-7469
Email: qian.wang@manhattan.edu

Hongbing Fang
Professor
Dept. of Mechanical Engineering & Engineering Science
The University of North Carolina at Charlotte
Charlotte, NC 28223
Tel: (704) 687-8328
Email: hfang@uncc.edu

Performing Organization(s):
Manhattan College
The University of North Carolina at Charlotte

Sponsor(s):
University Transportation Research Center (UTRC)

To request a hard copy of our final reports, please send us an email at utrc@utrc2.org

Mailing Address:

University Transportation Reserch Center
The City College of New York
Marshak Hall, Suite 910
160 Convent Avenue
New York, NY 10031
Tel: 212-650-8051
Fax: 212-650-8374
Web: www.utrc2.org

Board of Directors

The UTRC Board of Directors consists of one or two members from each Consortium school (each school receives two votes regardless of the number of representatives on the board). The Center Director is an ex-officio member of the Board and The Center management team serves as staff to the Board.

City University of New York
Dr. Hongmian Gong - Geography/Hunter College
Dr. Neville A. Parker - Civil Engineering/CCNY

Clarkson University
Dr. Kerop D. Janoyan - Civil Engineering

Columbia University
Dr. Raimondo Betti - Civil Engineering
Dr. Elliott Sclar - Urban and Regional Planning

Cornell University
Dr. Huaizhu (Oliver) Gao - Civil Engineering

Hofstra University
Dr. Jean-Paul Rodrigue - Global Studies and Geography

Manhattan College
Dr. Anirban De - Civil & Environmental Engineering
Dr. Matthew Volovski - Civil & Environmental Engineering

New Jersey Institute of Technology
Dr. Steven I-Jy Chien - Civil Engineering
Dr. Joyoung Lee - Civil & Environmental Engineering

New York University
Dr. Mitchell L. Moss - Urban Policy and Planning
Dr. Rae Zimmerman - Planning and Public Administration

Polytechnic Institute of NYU
Dr. Kaan Ozbay - Civil Engineering
Dr. John C. Falcocchio - Civil Engineering
Dr. Elena Prassas - Civil Engineering

Rensselaer Polytechnic Institute
Dr. José Holguín-Veras - Civil Engineering
Dr. William "Al" Wallace - Systems Engineering

Rochester Institute of Technology
Dr. James Winebrake - Science, Technology and Society/Public Policy
Dr. J. Scott Hawker - Software Engineering

Rowan University
Dr. Yusuf Mehta - Civil Engineering
Dr. Beena Sukumaran - Civil Engineering

State University of New York
Michael M. Fancher - Nanoscience
Dr. Catherine T. Lawson - City & Regional Planning
Dr. Adel W. Sadek - Transportation Systems Engineering
Dr. Shmuel Yahalom - Economics

Stevens Institute of Technology
Dr. Sophia Hassiotis - Civil Engineering
Dr. Thomas H. Wakeman III - Civil Engineering

Syracuse University
Dr. Riyad S. Aboutaha - Civil Engineering
Dr. O. Sam Salem - Construction Engineering and Management

The College of New Jersey
Dr. Thomas M. Brennan Jr - Civil Engineering

University of Puerto Rico - Mayagüez
Dr. Ismael Pagán-Trinidad - Civil Engineering
Dr. Didier M. Valdés-Díaz - Civil Engineering

UTRC Consortium Universities

The following universities/colleges are members of the UTRC consortium.

City University of New York (CUNY)
Clarkson University (Clarkson)
Columbia University (Columbia)
Cornell University (Cornell)
Hofstra University (Hofstra)
Manhattan College (MC)
New Jersey Institute of Technology (NJIT)
New York Institute of Technology (NYIT)
New York University (NYU)
Rensselaer Polytechnic Institute (RPI)
Rochester Institute of Technology (RIT)
Rowan University (Rowan)
State University of New York (SUNY)
Stevens Institute of Technology (Stevens)
Syracuse University (SU)
The College of New Jersey (TCNJ)
University of Puerto Rico - Mayagüez (UPRM)

UTRC Key Staff

Dr. Camille Kamga: *Director, Assistant Professor of Civil Engineering*

Dr. Robert E. Paaswell: *Director Emeritus of UTRC and Distin*guished Professor of Civil Engineering, The City College of New York

Herbert Levinson: *UTRC Icon Mentor, Transportation Consultant and Professor Emeritus of Transportation*

Dr. Ellen Thorson: *Senior Research Fellow, University Transportation Research Center*

Penny Eickemeyer: *Associate Director for Research, UTRC*

Dr. Alison Conway: *Associate Director for Education*

Nadia Aslam: *Assistant Director for Technology Transfer*

Nathalie Martinez: *Research Associate/Budget Analyst*

Tierra Fisher*: Office Assistant*

Bahman Moghimi*: Research Assistant;*
Ph.D. Student, Transportation Program

Wei Hao*: Research Fellow*

Andriy Blagay: *Graphic Intern*

TECHNICAL REPORT STANDARD TITLE PAGE

1. Report No.	2.Government Accession No.	3. Recipient's Catalog No.
4. Title and Subtitle A Probability-Based Approach for Assessment of Roadway Safety Hardware		5. Report Date 3/14/2017 6. Performing Organization Code
7. Author(s) Qian Wang, Hongbing Fang		8. Performing Organization Report No.
9. Performing Organization Name and Address Department of Civil and Environmental Engineering Manhattan College 4513 Manhattan College Parkway Bronx, NY 10471 Department of Mechanical Engineering & Engineering Science The University of North Carolina at Charlotte 9201 University City Blvd. Charlotte, NC 28223		10. Work Unit No. 11. Contract or Grant No. 49198-11-27
12. Sponsoring Agency Name and Address University Transportation Research Center Marshak Hall – Science Building, Suite 910 The City College of New York 138th Street & Convent Avenue, New York, NY 10031		13. Type of Report and Period Covered 14. Sponsoring Agency Code

15. Supplementary Notes

16. Abstract

This report presents a general probability-based approach for assessment of roadway safety hardware (RSH). It was achieved using a reliability analysis method and computational techniques. With the development of high-fidelity finite element (FE) models, numerical crash simulations can be performed to evaluate various RSH systems, in addition to crash tests. For highly nonlinear and implicit impact responses, metamodeling techniques provide a rational approach to replace the expensive numerical simulations. In this study, radial basis functions (RBFs) were employed to create approximation functions of limit state/performance functions using a relatively small number of sample points. Once the RBF metamodels were created, the failure probabilities were estimated using simulation methods such as Monte Carlo simulations (MCS). Based on the proposed approach, the failure probability can be obtained at different intensity measure (IM) levels, such as impact velocities. Effective use of numerical crash simulation and a metamodeling technique permits reliability analysis in an efficient manner and minimizes the number of required crash tests. As an application area, the assessment of a New Jersey concrete barrier was studied in this project to demonstrate the probability-based approach. Various crash responses and the corresponding response limits were selected and failure probabilities were calculated. The reliability analysis method will lead to the vulnerability analysis of RSH systems. It can be used to improve transportation safety, reduce the costs of RSH systems, and potentially replace the traditional pass/fail method widely used in practice.

17. Key Words reliability analysis, vulnerability, Monte Carlo Simulation (MCS), roadway safety hardware (RSH), finite element (FE), crash simulation, radial basis function (RBF)	18. Distribution Statement

19. Security Classif (of this report) Unclassified	20. Security Classif. (of this page) Unclassified	21. No of Pages 42	22. Price

Form DOT F 1700.7 (8-69)

Disclaimer

Table of Contents

List of Figures

List of Tables

1 ABSTRACT

This report presents a general probability-based approach for assessment of roadway safety hardware (RSH). It was achieved using a reliability analysis method and computational techniques. With the development of high-fidelity finite element (FE) models, numerical crash simulations can be performed to evaluate various RSH systems, in addition to crash tests. For highly nonlinear and implicit impact responses, metamodeling techniques provide a rational approach to replace the expensive numerical simulations. In this study, radial basis functions (RBFs) were employed to create approximation functions of limit state/performance functions using a relatively small number of sample points. Once the RBF metamodels were created, the failure probabilities were estimated using simulation methods such as Monte Carlo simulations (MCS). Based on the proposed approach, the failure probability can be obtained at different intensity measure (IM) levels, such as impact velocities. Effective use of numerical crash simulation and a metamodeling technique permits reliability analysis in an efficient manner and minimizes the number of required crash tests. As an application area, the assessment of a New Jersey concrete barrier was studied in this project to demonstrate the probability-based approach. Various crash responses and the corresponding response limits were selected and failure probabilities were calculated. The reliability analysis method will lead to the vulnerability analysis of RSH systems. It can be used to improve transportation safety, reduce the costs of RSH systems, and potentially replace the traditional pass/fail method widely used in practice.

Keywords: *reliability analysis, vulnerability, Monte Carlo Simulation (MCS), roadway safety hardware (RSH), finite element (FE), crash simulation, radial basis function (RBF)*

2 INTRODUCTION

The ever-increasing traffic volumes on state and local highways have raised more public concerns on transportation safety. Vehicular crashes at high speeds usually lead to significant social and economic loss, in addition to loss of occupant lives. RSH systems shall be designed to redirect an impacting vehicle so that a rollover or a second crash with other vehicles is prevented. Therefore they can be effective in minimizing the injuries to occupants in a vehicle. Over the years, different types of RSH systems have been designed and installed in order to reduce the severity of vehicle crashes. These include roadside or median barriers, guardrails, bridge rails, terminals, and crash cushions. Historically, the vehicle crashworthiness and performance of RSH systems have been evaluated using limited full-scale crash testing and in-service performance. The proposed research project focused on the development of a reliability analysis and safety evaluation method for RSH systems using computational techniques.

For commonly used RSH systems, improving the design methodology from a prescriptive pass/fail method to a probability-based method is an important task for highway safety research. Very limited research is found in literature that aims to develop probability-based approaches or analytical models for assessing the vulnerability of RSH systems subjected to vehicle crashes. Such approaches or analytical models are essential to the understanding of vehicle crashes and RSH failures as well as to designing and retrofitting RSH systems. Due to the limitations of physical testing, there is a need to perform reliability analysis using numerical crash simulations so that various levels of vehicle crashes can be considered.

Engineering vulnerability analysis is primarily based on reliability analysis methods which are used to calculate the failure probability of a given engineering system. Therefore the level of safety of the system can be evaluated. A probabilistic description of the crash failures and vulnerability of RSH systems subjected to vehicle crashes is described by an impact IM. The IM is an attribute of a vehicle impact that can be used to describe the level of impact severity and potential failures for a given RSH system, such as impact velocity or impact angle of the vehicle. The most commonly used reliability analysis methods in literature fall into two categories: most probable point (MPP) and sampling methods. The MPP-based methods are widely used for structural and mechanical systems, when combined with simulation or analysis methods such as the FE methods. These include first-order reliability methods (FORM) and second-order reliability methods (SORM). Since first-order derivatives of simulation responses or outputs are required, the integration of the MPP methods with an available FE code is usually not straightforward, especially for complicated nonlinear problems. In the sampling methods, the random variables are sampled and the limit state/performance function is evaluated at all sample points. Since derivative calculations are not required in the sampling methods, sensitivity analyses of the limit state function in terms of the random variables can be avoided. Moreover, an FE analysis code is routinely treated as a black-box program in a sampling method. It is very straightforward to implement the method, although it is not efficient, especially when a large number of numerical analyses are needed. In this case, it becomes computationally prohibitive to combine a sampling approach with expensive numerical simulations.

2.1 *Research Objectives*

In this study, a general probability-based analysis framework for assessing the RSH design and performance was developed. The probability of RSH failures under vehicular impacts was investigated using post-impact vehicle responses, such as velocities and accelerations. This research used computational techniques to develop a basic understanding and foundation for a much needed analytical model for the vulnerability analysis of RSH systems under vehicular impacts (i.e., crash magnitudes vs. RSH failure probability). The research is intended to improve engineering practice in the field of transportation safety and decision-making. This is different from the current deterministic approach which uses a prescribed pass/fail criterion based on "representative" or average conditions. The results of the proposed research will lead to optimum engineering solutions for the cost-effective installation and retrofit of various RSH systems.

2.2 *Research Methodology*

The research project studied vehicle-RSH impacts and investigated vehicle as well as occupant responses. In most physical tests, crash dummies are not used. Evaluation criteria that are directly based on occupant injuries are not commonly considered. Therefore, the occupant safety and injuries are evaluated primarily based on responses of the vehicle alone. In this study, a physics-based numerical simulation method and a probability-based approach were combined in order to develop a general reliability analysis method that will be useful for transportation safety study. To reduce computational efforts, a metamodeling technique was developed. The RBFs or augmented RBFs were used to construct explicit metamodels of the crash responses and limit state functions. After the explicit form of a limit state function was obtained, the MCS method was applied to estimate the failure probability. The methodology developed in this study can be applied to RSH systems under different crash conditions. As a sample application area, the proposed method was applied to the reliability analysis of New Jersey concrete barriers. The general methodology was demonstrated and multiple limit state functions involving vehicle and occupant responses were considered. A pickup truck specified by the current crash standard was adopted in the nonlinear crash simulations.

2.3 *Report Organization*

In the remainder of the report, some background research including a review of literature and safety evaluation of RSH systems is reviewed in Section 3. Details of the numerical simulations are introduced in Section 4. The FE models of a pickup truck and concrete barrier and validation of the numerical models are presented. Existing crash test data available in the literature were used for model validation. Section 5 of the report presents details of the probability-based analysis method. A metamodeling method and the overall flowchart of the approach are introduced. The metamodeling technique based on RBFs and augmented RBFs is explained, and it was used to create explicit nonlinear crash response functions. As an application area, the concrete barrier problem is introduced in Section 6. The limit state functions and the reliability analysis results are presented. Concluding remarks are given in Section 7. Finally, some future research topics are summarized in Section 8.

3 BACKGROUND RESEARCH

3.1 *Literature Review and State of Practice*

3.1.1 *RSH design and testing*

Highway safety research, which involves vehicle crashes, usually focuses on the design and evaluation of RSH systems that prevent vehicles from rollover, crashing into other vehicles, or entering undesirable regions. Over the years, various RSH systems have been developed and installed in order to reduce vehicle crashes. Figure 1. Commonly-used RSH systems [1-4]. shows three commonly-used RSH systems in the U.S., including concrete, W-beam, and cable barriers [1-4]. Although these barriers are generally effective, there remains significant room for improvement. To verify the crash behaviors of the RSH systems, full-scale physical crash tests have been conducted in prescribed conditions that should be representative of the service installation. The document entitled "*The Highway Research Correlation Services Circular 482*" was the first published document for crash tests and evaluation of the performance of RSH systems [5]. The National Cooperative Highway Research Program (NCHRP) adopted the NCHRP Report 350 in 1993 [6], which is a safety standard for roadside safety in the U.S. The NCHRP Report 350 specifies the testing and evaluation criteria for RSH systems before they can be installed on highways. Numerous studies have been conducted since then to evaluate different types of barriers as well as other highway safety features using physical crash tests [7-20].

a. b. c.

Figure 1. Commonly-used RSH systems [1-4].
a. a concrete barrier; b. a W-beam guardrail; and c. a cable barrier.

An updated safety guideline, the *Manual for Assessing Safety Hardware* (MASH), was published by the American Association of State Highway & Transportation Officials (AASHTO) in 2009 [21]. Full-scale crash tests were conducted under MASH TL-3 conditions at the Midwest Roadside Safety Facility (MwRSF) [22-28] and the Texas Transportation Institute (TTI) [29-33]. In these physical tests, various types of barriers and guardrails were studied. A concrete bridge rail was designed and tested under the impact of a single unit truck to meet the MASH TL-4 conditions. The FE model of the truck was validated based on the test data [34]. Some other full-scale physical crash tests on RSH systems can also be found in the literature [35-38], including testing under MASH TL-5 conditions [36] and the special condition of missing a post of longitudinal barriers [37].

Although physical crash tests are commonly used to obtain valuable information on vehicular impact behavior, they are primarily used for limited validation purposes. The evolution of new computer hardware and software technology has promoted the usage of explicit FE codes such as LS-DYNA in crash analyses [39]. It becomes affordable and popular to rely on full-scale FE simulations to study vehicular crashes [40-46]. In addition, FE models of various vehicles [47-53] and RSH systems [54, 55] were developed. Due to the efficiency and effectiveness of numerical simulations, they have been widely adopted to aid the performance evaluation and improvement of various RSH systems [56-85].

3.1.2 *Simulation-based optimization and reliability analysis*

Using numerical simulations, optimal designs and reliability analysis of complex engineering problems can be performed in an effective manner. In the automotive industry, numerous studies have been performed on crashworthiness design and optimization of vehicular components and structures [86-95]. In the transportation safety field, simulation-based design optimization has not been widely developed and adopted in RSH designs. Recently, Hou et al. [96, 97] and Yin et al. [98] studied design optimization of different median barrier systems under vehicle crashes.

Although MCS can be used to provide relatively accurate assessment of the system performance or reliability, this method is computationally very expensive, and often unaffordable, when combined with high-fidelity nonlinear FE models to obtain system responses. This is because MCS would require a large number of computationally expensive analyses to obtain sufficiently accurate results [99]. Alternatively, FORM and SORM can be adopted to provide relatively efficient computational solutions for estimating the reliability of a structural system [100]. However, both FORM and SORM involve system sensitivity analyses that require the gradients of a structural response. Given the implicit nature of the structural responses in a numerical analysis, the finite difference approximation is commonly used in the sensitivity analysis [101], but it can be expensive as well due to the additional simulations required to calculate the gradients. For the above-mentioned challenges of the three methods for reliability analysis, there is a need to adopt a more efficient approach to conducting reliability analysis.

Over the past decades, performance-based analysis and design methods have been extensively developed in civil and structural engineering [102-106], especially in earthquake engineering [102-104]. In a performance-based analysis, the system response is described in terms of engineering demand parameters and is evaluated according to different IM levels (e.g., earthquake intensity). The system performance is evaluated by comparing the structural response to appropriate damage measures, which are used to determine the levels of physical damage [102]. The structural reliability analysis and the performance-based approaches have led to reliability-based optimal designs of structures [107, 108]. Among the tools developed in probabilistic methods, the construction of fragility curves has attracted considerable interest in the research community, especially earthquake engineering [109-114]. Fragility describes the ability of an engineering system or component to withstand a specified event. A fragility curve is a statistical tool representing the cumulative probability of the engineering demand placed upon the system exceeding its capacity. This represents failure with respect to a specific limit or failure state for a given IM level [112].

3.1.3 *Metamodeling methods*

In simulation-based reliability analysis, a large number of numerical analyses are generally required. The highly nonlinear impact simulations are computationally very expensive, because the simulations involve large deformations, material failures and a large number of contact analyses. This brings significant challenges to reliability analysis using MCS directly [99]. To improve the computational efficiency yet maintain the complex features of modeling, various metamodeling approaches have been studied and become available in the reliability analysis of structural and mechanical systems involving expensive simulations.

To meet the challenges in simulation-based reliability analysis, a rational approach is to replace the expensive numerical simulations (used to obtain structural responses) with inexpensive yet accurate metamodels or surrogate models. For each structural response, a metamodel can be constructed using results of prescribed simulations for a certain number of input conditions. The advantages of metamodels are that they are in explicit mathematical forms with readily available gradient functions, beside their high efficiency in obtaining a structural response compared to the numerical simulations. The most popular metamodel is the response surface method (RSM). The RSM uses the least-square polynomial regression model, which is efficient and simple to use; it has been widely applied in many practical problems including engineering reliability analysis [115-121], design optimization [122-124], and reliability-based design optimization [125, 126]. To improve the accuracy of RSM models used in reliability analysis, different techniques were proposed such as the vector projection sampling techniques [117], resampling techniques [118], and higher order effects in the response function [119, 120]. However when a single global RSM model is used for the entire response space, large errors may be introduced in the approximation, especially when highly nonlinear functions are considered. To improve model accuracy, local RSM methods were proposed. The moving least squares technique was applied in reliability analysis to deal with highly nonlinear responses [121]; however, these local approaches can only represent a small region of the entire response space. Other metamodeling approaches are also available to approximate implicit functions, for example, kriging [127, 128], artificial neural networks [129, 130], high-dimensional model representation (HDMR/FHDMR) [131-133], and RBFs [134, 135].

The RBFs were originally used to fit irregular geographical data [136]. Recent studies showed that the RBFs could create better approximation models compared to other global methods such as the global RSM for highly nonlinear responses [137, 138]. One advantage of RBFs is that RBF metamodels have no errors on the sample points. Many different basis functions were studied by Fang et al. [139, 140]. These functions included Gaussian, multiquadric, as well as Wu's compactly supported (CS) basis functions [141]. In these studies, the CS basis functions were used to generate metamodels of different responses, including linear and highly nonlinear mathematical and engineering functions. Several accurate basis functions were identified. For all test functions, the augmented RBF metamodels based on CS basis functions were shown to have better accuracy than their respective non-augmented models. Multiobjective optimization of complex structures including crashworthiness design was successfully solved using metamodels created based on augmented RBFs [138-140].

3.2 *Safety Evaluation of RSH Systems*

3.2.1 *Vehicle responses based on MASH*

In the U.S., RSH systems should be tested and evaluated to meet the MASH requirements [21]. MASH specifies a total of six test levels (TL). The MASH TL-3 conditions, which are listed in Table 1, were employed in this study. This is the commonly used TL by State Departments of Transportation (DOTs). In Table 1, 1100C represents a small passenger car of 1100 kg. Test designation 3-11 requires a 2270P vehicle which refers to a 2270-kg pickup truck. In this study, only 2270P was used for numerical simulations and reliability analyses. However the proposed reliability analysis method is general and can be applied to any other vehicles with different crash conditions.

Table 1. TL-3 conditions in MASH [21].

Test designation	Test vehicle	Impact velocity (km/h)	Impact angle (degree)
3-10	1100C	100	25
3-11	2270P	100	25

The performance of an RSH system under vehicular impacts is evaluated using different criteria. According to MASH, the three criteria are "*the risk of injury to the occupants of the impacting vehicle*," "*the structural adequacy of the safety feature*" and "*the post-impact behavior of the test vehicle*" [21]. The "structural adequacy of the safety feature" is not a major concern for concrete barriers. The post-impact vehicular behaviors include various impact angles and velocities of the vehicle. Besides the maximum yaw, pitch, and roll angles of a vehicle, the vehicle's exit angle (EA) is also an important measure for evaluating RSH systems. The maximum roll angle and the vehicle's EA are related to the vehicle's rollover and safe redirection, respectively. Figure 2 illustrates the conditions of a vehicle impacting a median barrier, including the impact angle, exit angle, and the impact velocity (v = 100 km/h is shown here). Figure 3 defines the yaw, pitch, and roll angles of a vehicle.

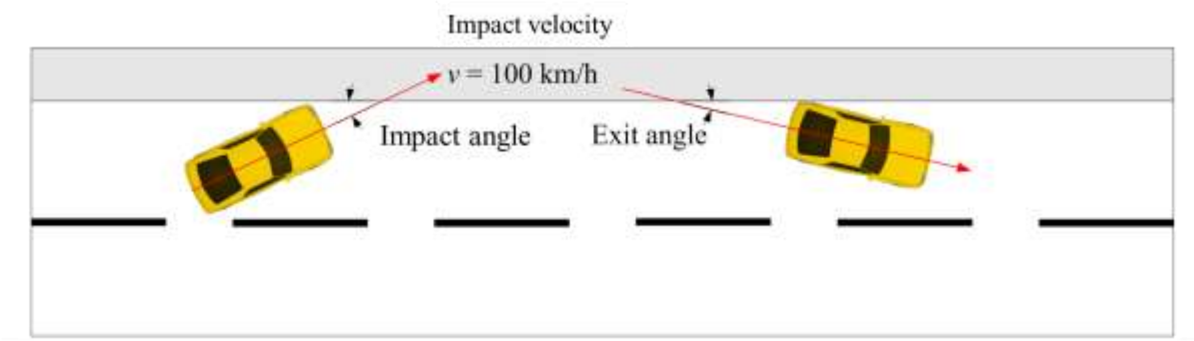

Figure 2. Illustration of impact conditions.

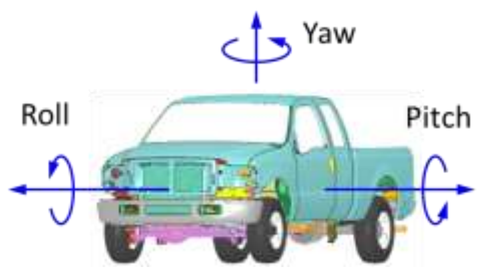

Figure 3. Yaw, pitch, and roll angles of a vehicle [85].

3.2.2 *Occupant injury criteria based on vehicle responses*

In order to evaluate occupant responses, crash dummies can be adopted. However, they are not specified by MASH and have not been widely included in crash tests and simulations. The occupant injuries are evaluated mainly based on responses of the impacting vehicle. During a crash, the crash responses including impact forces, velocities, and accelerations can be used to quantify the severity of an impact. Furthermore, the occupant injury risk is correlated to severity of impact and vehicular responses [142]. MASH uses the flail space model to evaluate the impact severity and injuries [143]. Two major responses can be used, i.e., occupant impact velocity (OIV) and occupant ridedown acceleration (ORA). The OIV represents the hypothetical occupant-vehicle impact velocity, and it is a relative velocity. The OIV in the longitudinal and lateral directions are

$$\mathrm{OIV}_x = \int_0^{t_0} a_x dt \quad (1)$$

$$\mathrm{OIV}_y = \int_0^{t_0} a_y dt \quad (2)$$

In Eqs. (1) and (2), a_x and a_y are the accelerations of the vehicle in the two directions, respectively. t_x and t_y represent the times of free motions of the hypothetical occupant in the two directions, respectively. The time of free motions $t_0 = \min\{t_x, t_y\}$. To determine t_x and t_y, the following equations are solved:

$$\int_0^{t_x} dt \int_0^{t_x} a_x dt = 0.6 \tag{3}$$

$$\int_0^{t_y} dt \int_0^{t_y} a_y dt = 0.3 \tag{4}$$

The acceptable and preferred maximum OIV values specified in MASH are 12.2 m/s and 9.1 m/s, respectively. The ORA represents the greatest 10-ms average acceleration of the hypothetical occupant during the subsequent ridedown after t_0. According to MASH, the acceptable and preferred maximum ORA values are 20.49 *g* and 15.0 *g*, respectively. The gravitational acceleration is denoted by *g*.

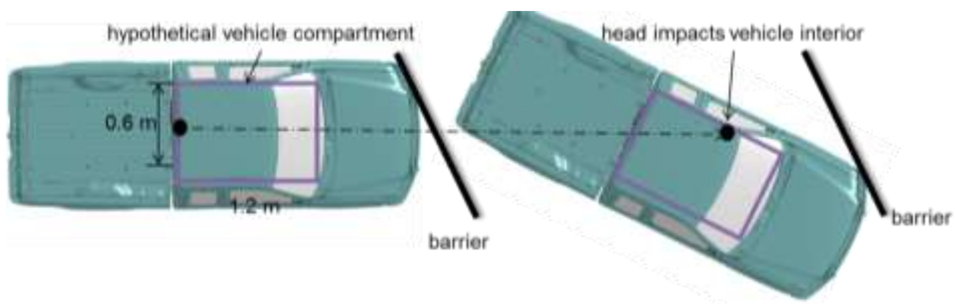

a.

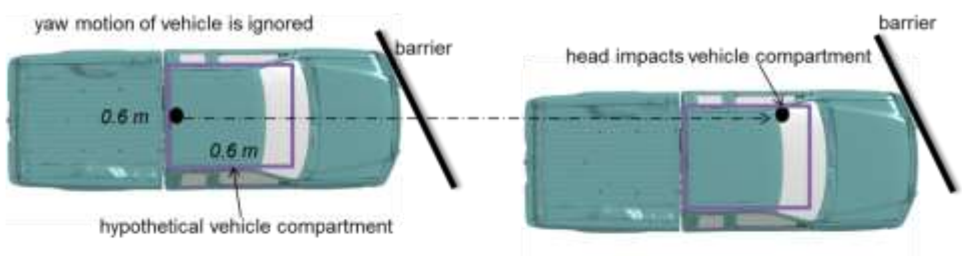

b.

Figure 4. Illustration of occupant injury concepts [85].
a. THIV and b. OIV.

Besides OIV and ORA, the acceleration severity index (ASI), post-impact head deceleration (PHD), and the theoretical head impact velocity (THIV) can also be used to evaluate occupant risks in a vehicular crash. These criteria are adopted by the European Committee for Normalization (CEN), but only recommended in MASH. The larger these values are, the higher the occupant risk to injury. The ASI can be calculated as

$$ASI(t) = \left[\left(\frac{\bar{a}_x}{\hat{a}_x} \right)^2 + \left(\frac{\bar{a}_y}{\hat{a}_y} \right)^2 + \left(\frac{\bar{a}_z}{\hat{a}_z} \right)^2 \right]^{\frac{1}{2}} \tag{5}$$

where $\bar{a}_x$, $\bar{a}_y$, $\bar{a}_z$ are the average accelerations in 50-*ms* and $\hat{a}_x$ = 12 *g*, $\hat{a}_y$ = 9 *g*, and $\hat{a}_z$ = 10 *g* are the threshold accelerations of vehicle, respectively. The PHD is the maximum resultant acceleration filtered and averaged over a 10-*ms* period. The THIV and OIV have similar concepts, as can be seen from Figure 4. To determine THIV, the yaw motion is included and a 1.2 × 0.6 *m* rectangular space in the vehicle interior is considered.

4 FINITE ELEMENT ANALYSIS AND VALIDATION

4.1 *Finite Element Analysis*

In this study, a 2007 Chevy Silverado pickup truck was selected, which met the MASH TL-3 requirements. LS-DYNA software was used for the explicit transient dynamic impact analyses. Figure 5 shows the FE models of the pickup truck, one with mesh and one without mesh. The FE model of the truck was developed at the National Crash Analysis Center (NCAC). It was initially validated based on the data obtained from full frontal crash and other tests [144-147].

a. b.

Figure 5. The FE models of a 2007 Chevy Silverado pickup (2270P).
a. without mesh and b. with mesh [98].

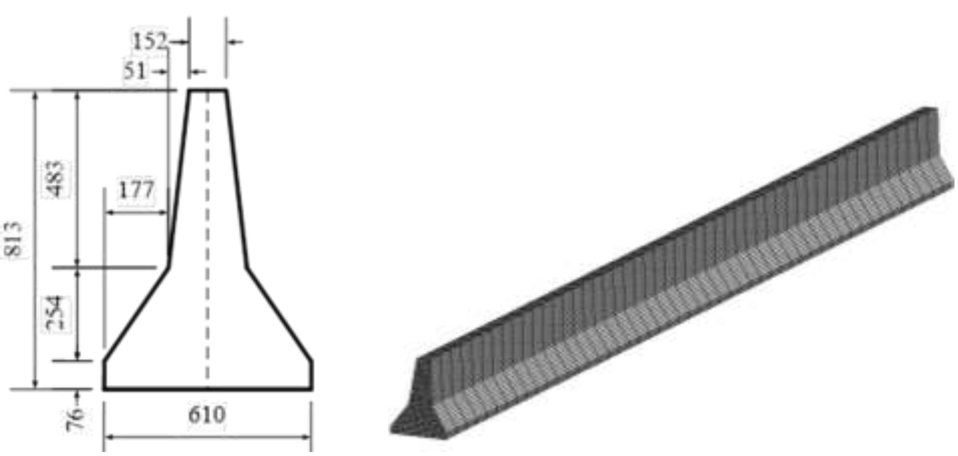

a. b.

Figure 6. The New Jersey concrete barrier.
a. cross-section and b. the FE model [98].

The New Jersey concrete barrier (Jersey barrier) is widely used in the U.S. and was selected in this study. The cross-section of the Jersey barrier and its FE model are shown in Figure 6. The FE model of the Jersey barrier was also originally developed at NCAC. The Jersey barrier was set to be 20 m long. The concrete barrier was treated as rigid, and the rigid material MAT20 was assigned to the barrier. It is a common practice to model concrete barriers as completely rigid [55, 82], since they generally have insignificant deformation under vehicular impacts. The base of the concrete barrier was fixed in the FE model, so displacements were not allowed in a crash.

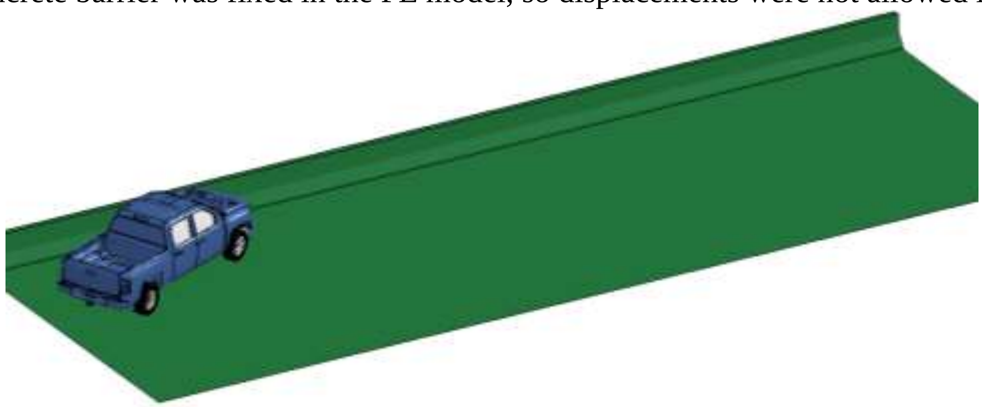

Figure 7 shows the model of the entire barrier and vehicle system.

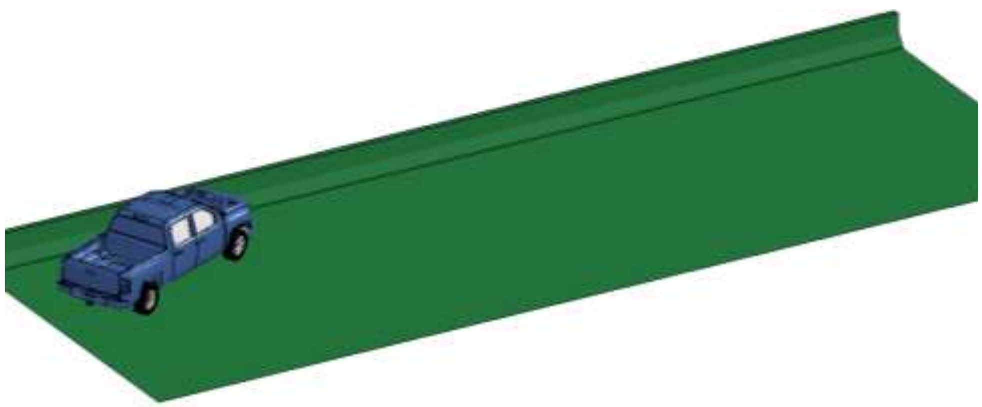

Figure 7. The FE model of the entire concrete barrier and vehicle system [98].

4.2 *Model Validation*

The FE models were validated against existing test data to ensure accurate results. Before the models were used in reliability analyses, the vehicle and concrete barrier models were further validated using full-scale crash test results from the literature [82]. Figure 8 show a visual comparison between the physical test data and the vehicular responses obtained using numerical simulations. Similar vehicular responses were observed in the computer simulation and the physical crash test at various time steps. The comparisons of the yaw and roll angles are given in Figure 9. Both the test data and FE analysis results are shown. It was found that the test data and analysis results have a good agreement [98]. It was concluded that the FE models were appropriate for impact simulations in this study.

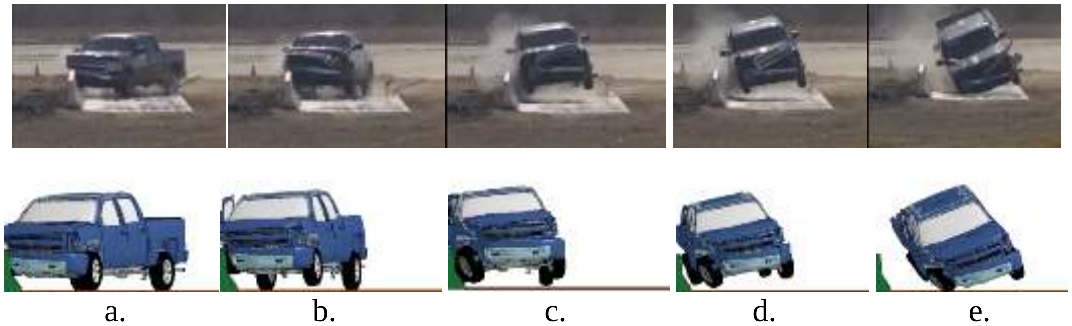

Figure 8. Visual comparison of crash test and simulated vehicle responses [98].
a. *t = 50 ms*, b. *t = 105 ms*, c. *t = 180 ms*, d. *t = 265 ms*, and e. *t = 475 ms*.

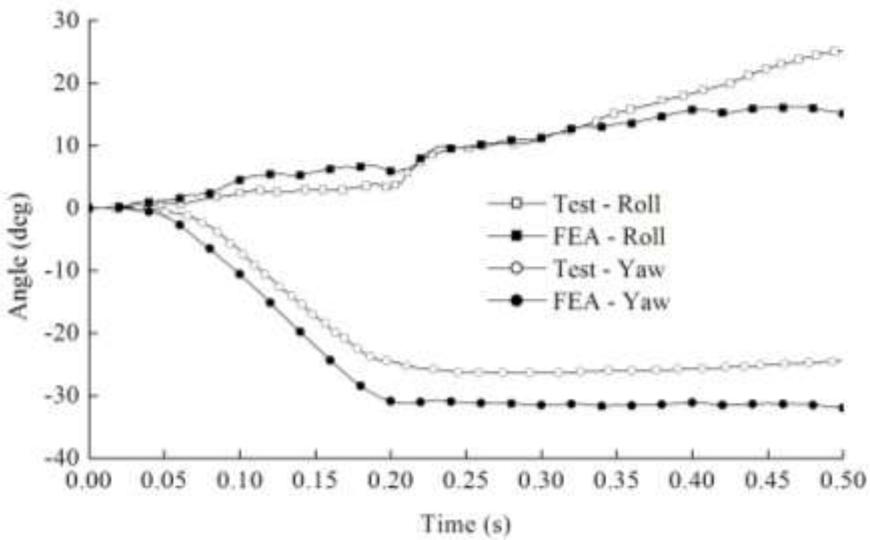

Figure 9. Comparison of both yaw and roll angles between FE analysis and test data [98].

5 A PROBABILITY-BASED ANALYSIS METHOD

5.1 *A Probability-Based Analysis Framework*

In the proposed research, a probability-based analysis method was studied. This will be eventually used to develop a probabilistic analytical model for assessing the failure of RSH due to vehicle crashes. The new analysis method will provide a probabilistic description of the crash failures of an RSH system subjected to vehicle crashes described by IMs. The IMs are a set of attributes of a vehicle impact that can be used to describe the level of impact severity and potential failures of a given RSH system, such as impact velocity or angle of the vehicle. In the analysis, an RSH performance index or failure index (*FI*) is first determined and expressed as a function of the RSH capacity (*R*) and crash responses (*P*), i.e., $FI = f(R,P)$. For each IM or each set of IMs, the crash failure levels of RSH are determined by comparing the *FI* to the corresponding RSH crash failure criteria. The probability of failure is calculated. Figure 10 shows the general framework of stochastic RSH crash analysis.

5.2 *Engineering Reliability Analysis*

In an engineering reliability analysis, the probability of failure of a component or system can be evaluated. Calculation of the failure probability, P_F, involves the following multidimensional probability integrals [148, 149]:

$$P_F \equiv P(g(\mathbf{x}) \leq 0) = \int_{g(\mathbf{x})\leq 0} p_X(\mathbf{x}) d\mathbf{x} \tag{6}$$

where $\mathbf{x}$ is an k-dimensional random variable vector, $g(\mathbf{x})$ is a limit state function, and $p_x(\mathbf{x})$ is the joint probability density function (PDF) of vector $\mathbf{x}$, respectively. $g(\mathbf{x}) \leq 0$ is defined as failure of the component or system. In many practical applications, $p_x(\mathbf{x})$ is unknown. In addition, Eq. (6) is difficult to obtain since $g(\mathbf{x})$ is an implicit function of $\mathbf{x}$. Simulations of an engineering system, such as nonlinear FE analyses, are required to be integrated with a reliability analysis method. The function $g(\mathbf{x})$ is often transformed into a standard Gaussian space and approximated using the first-order or second-order Taylor series expansion in FORM or SORM, respectively [149, 150].

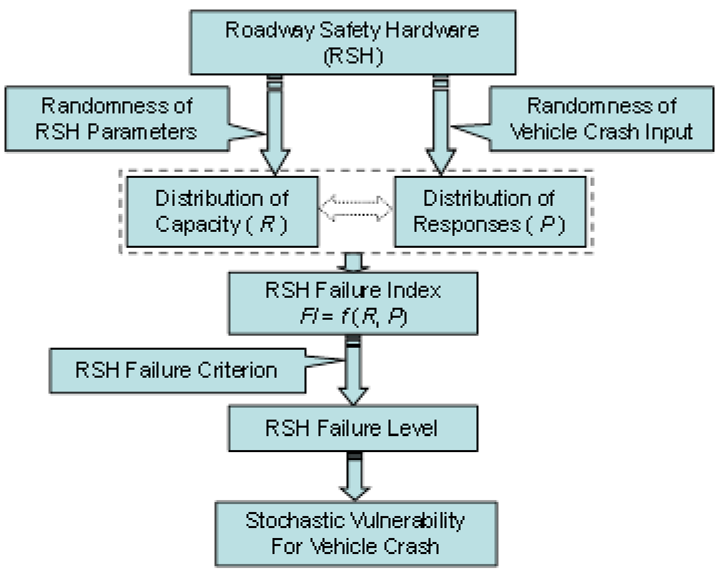

Figure 10. A general framework of stochastic crash analysis.

5.3 *A Metamodeling Technique Based on RBFs*

Consider an input-output response function as follows

$$z = g(\mathbf{x}) \tag{7}$$

where $\mathbf{x} = [x_1, \ldots x_k]$ is a design or input variable vector, and z is the output of function $g(\mathbf{x})$. In many engineering problems, an explicit form of $g(\mathbf{x})$ is unknown. However, $g(\mathbf{x})$ can be evaluated using numerical simulations for any input $\mathbf{x}$. The basic concept of a metamodel is to create an approximate but explicit expression of $g(\mathbf{x})$.

Before a metamodel of function $g(\mathbf{x})$ is created, the function value needs to be evaluated at some sample points, so that the entire input space is well represented. This is typically conducted using a *design of experiments* (DOE) method, such as Latin hypercube method [151], factorial design, and Taguchi method [152]. With the function values at a total of n sample points, metamodels can be created using RBFs, as

$$\tilde{g}(\mathbf{x}) = \sum_{i=1}^{n} \lambda_i \phi(\|\mathbf{x} - \mathbf{x}_i\|) \tag{8}$$

where ϕ and λ_i are the RBF basis function and the weighted coefficient for the ith basis function, respectively. $\mathbf{x}_i$ and $\| \mathbf{x} - \mathbf{x}_i \|$ are the input variable vector and Euclidean norm. The RBF metamodel as written in Eq. (8) is essentially a linear combination of radial basis functions constructed around each sample point. A number of basis functions were examined, including some commonly used functions and the CS functions [139]. These are listed in Table 2.

Table 2. Commonly used radial basis functions [139].

Name	Symbol	Radial basis function
Linear	RBF-LN	$\phi(r) = r$
Cubic	RBF-CB	$\phi(r) = r^3$
Thin-plate spline	RBF-TPS	$\phi(r) = r^2 \ln(cr),\ 0 < c \le 1$
Gaussian	RBF-GS	$\phi(r) = e^{-cr^2},\ 0 < c \le 1$
Multiquadric	RBF-MQ	$\phi(r) = \sqrt{r^2 + c^2},\ 0 < c \le 1$
Inverse multiquadric	RBF-IMQ	$\phi(r) = \frac{1}{\sqrt{r^2 + c^2}},\ 0 < c \le 1$
Compactly supported (2,0)	RBF-CS20	$\phi_{2,0}(t) = (1-t)^5(1 + 5t + 9t^2 + 5t^3 + t^4), \quad \mathrm{t} = \mathrm{r}/\mathrm{r}_0$
Compactly supported (2,1)	RBF-CS21	$\phi_{2,1}(t) = (1-t)^4(4 + 16t + 12t^2 + 3t^3)$
Compactly supported (2,2)	RBF-CS22	$\phi_{2,2}(t) = (1-t)^3(8 + 9t + 3t^2)$
Compactly supported (3,0)	RBF-CS30	$\phi_{3,0}(t) = (1-t)^7(5 + 35t + 101t^2 + 147t^3 + 101t^4 + 35t^5 + 5t^6)$
Compactly supported (3,1)	RBF-CS31	$\phi_{3,1}(t) = (1-t)^6(6 + 36t + 82t^2 + 72t^3 + 30t^4 + 5t^5)$
Compactly supported (3,2)	RBF-CS32	$\phi_{3,2}(t) = (1-t)^5(8 + 40t + 48t^2 + 25t^3 + 5t^4)$
Compactly supported (3,3)	RBF-CS33	$\phi_{3,3}(t) = (1-t)^4(16 + 29t + 20t^2 + 5t^3)$

A total of n equations can be written by replacing $\mathbf{x}$ and $\tilde{g}(\mathbf{x})$ in Eq. (8) with the n input variable vectors at the sample points and corresponding function values, as

$$\tilde{g}(\mathbf{x}_1) = \sum_{i=1}^{n} \lambda_i \phi(\|\mathbf{x}_1 - \mathbf{x}_i\|)$$

$$\tilde{g}(\mathbf{x}_2) = \sum_{i=1}^{n} \lambda_i \phi(\|\mathbf{x}_2 - \mathbf{x}_i\|)$$

…

$$\tilde{g}(\mathbf{x}_n) = \sum_{i=1}^{n} \lambda_i \phi(\|\mathbf{x}_n - \mathbf{x}_i\|) \tag{9}$$

To write Eq. (9) in a matrix form, as

$$\tilde{\mathbf{g}} = \mathbf{A}\boldsymbol{\lambda} \tag{10}$$

where $\tilde{\mathbf{g}} = [\tilde{g}(\mathbf{x}_1) \quad \tilde{g}(\mathbf{x}_2) \quad ... \quad \tilde{g}(\mathbf{x}_n)]^T$, $A_{i,j} = \phi(\|\mathbf{x}_i - \mathbf{x}_j\|)$ (i = 1, … n, j = 1, … n), and $\boldsymbol{\lambda} = [\lambda_1, \ldots \lambda_n]^T$. The coefficients $\boldsymbol{\lambda}$ can be calculated by solving Eq. (9).

The RBF metamodel in Eq. (8) is generally appropriate for approximating nonlinear responses, since highly nonlinear basis functions are adopted. However, they were found to be less accurate to approximate linear functions [137]. To make RBFs suitable for both high-order and low-order responses, augmented RBF models can be defined by adding linear or quadratic functions to Eq. (8), as

$$\tilde{g}(\mathbf{x}) = \sum_{i=1}^{n} \lambda_i \phi(\|\mathbf{x} - \mathbf{x}_i\|) + \sum_{j=1}^{p} c_j f_j(\mathbf{x}) \tag{11}$$

where $f(\mathbf{x})$ is a polynomial function. In the second part of Eq. (11), p and c_j (j = 1,… p) represent the total number of terms and the coefficients in the polynomial, respectively. Because there are more unknowns than available equations, Eq. (11) is underdetermined. Therefore, the following orthogonality condition is required

$$\sum_{i=1}^{n} \lambda_i f_j(\mathbf{x}_i) = 0, \quad \text{for } j = 1,...p \tag{12}$$

Equations (11) and (12) result in a total of (n+p) equations. To write the matrix form of these equations, as

$$\begin{pmatrix} \mathbf{A} & \mathbf{F} \\ \mathbf{F}^{\mathbf{T}} & \mathbf{0} \end{pmatrix} \begin{pmatrix} \boldsymbol{\lambda} \\ \mathbf{c} \end{pmatrix} = \begin{pmatrix} \mathbf{g} \\ \mathbf{0} \end{pmatrix} \tag{13}$$

where $F_{i,j} = f_j(\mathbf{x}_i)$ (i = 1, … n, j=1, … p) and $\boldsymbol{c}=[c_1, \ldots c_p]^T$. Coefficients $\boldsymbol{\lambda}$ and $\boldsymbol{c}$ for the augmented RBF model in Eq. (11) can be found by solving Eq. (13).

For ease of discussion, an augmented RBF metamodel is expressed based on the symbol for its corresponding non-augmented metamodel with a suffix '-LP' if a linear polynomial is considered or '-QP' if a quadratic polynomial is added. One of the RBF models created using compactly supported function CS20 augmented with linear polynomials was found to have good accuracy; therefore, it was used in this study, namely RBF-CS20-LP. The RBF and augmented RBF metamodels have explicit mathematical forms; therefore their function values can be very efficiently calculated. Another advantage of these metamodels is that all the required simulations at the sample points can be performed concurrently using parallel computation. Therefore the simulation time can be greatly reduced if a large sample of expensive simulations is required.

To measure the accuracy of metamodels, the Analysis of Variance (ANOVA) may be used and the errors at sample points are needed. These errors are zeroes for RBF metamodels; therefore, ANOVA does not provide useful insight into the accuracy of RBF metamodels. Instead, the root mean square errors (RMSEs) can be used to assess the accuracy of RBF metamodels [140], as

$$\mathrm{RMSE} = \sqrt{\frac{\sum_{i=1}^{k} (g_i - \tilde{g}_i)^2}{k}} \tag{14}$$

Here a total number of *k* off-sample points are randomly generated. In Eq. (14), g_i is the true function value and $\tilde{g}_i$ represents the metamodel function value evaluated at the i^{th} off-sample point, respectively.

5.4 *Estimation of Failure Probability*

Equations (8) and (11) provide approximation function $\tilde{g}(\mathbf{x})$ of $g(\mathbf{x})$ using an RBF and augmented RBF metamodel, respectively. When MCS are applied based on the RBF metamodel $\tilde{g}(\mathbf{x})$, Eq. (6) becomes:

$$P_F \equiv P(g(\mathbf{x}) \le 0) = \frac{1}{N} \sum_{i=1}^{N} \Gamma\left[\tilde{g}\left(\mathbf{x}^i\right) \le 0\right] \tag{15}$$

where *N* is the MCS sample size, $\mathbf{x}^i$ is the i^{th} realization of $\mathbf{x}$, and Γ is a deciding function such that $\Gamma = 1$, if $\tilde{g}\left(\mathbf{x}^i\right) \le 0$, and $\Gamma = 0$ if $\tilde{g}\left(\mathbf{x}^i\right) > 0$. Based on the failure probability P_F, the reliability index β can be determined by [131, 132]:

$$\beta = -\Phi^{-1}\left(P_F\right) \tag{16}$$

where Φ is the cumulative distribution function (CDF) of a standard Gaussian random variable. The coefficient of variation δ used in MCS can be estimated as [131, 132]:

$$\delta = \sqrt{\frac{\left(1 - P_F\right)}{N P_F}} \tag{17}$$

where *N* is the sample size of the MCS method and P_F is the failure probability, respectively.

5.5 *Overall Flowchart*

Figure 11 shows a flow chart of reliability analysis using RBF metamodels. Once an explicit RBF metamodel is constructed, the failure probability, P_F, can be estimated using any sampling method. In this study, the MCS method was applied. It is important to note that the number of expensive FE simulations depends on the sample size to create an RBF metamodel, rather than the sample size used in MCS. The computational cost is primarily from FE analyses and evaluations of function $g(\mathbf{x})$, i.e., original implicit response simulations [153].

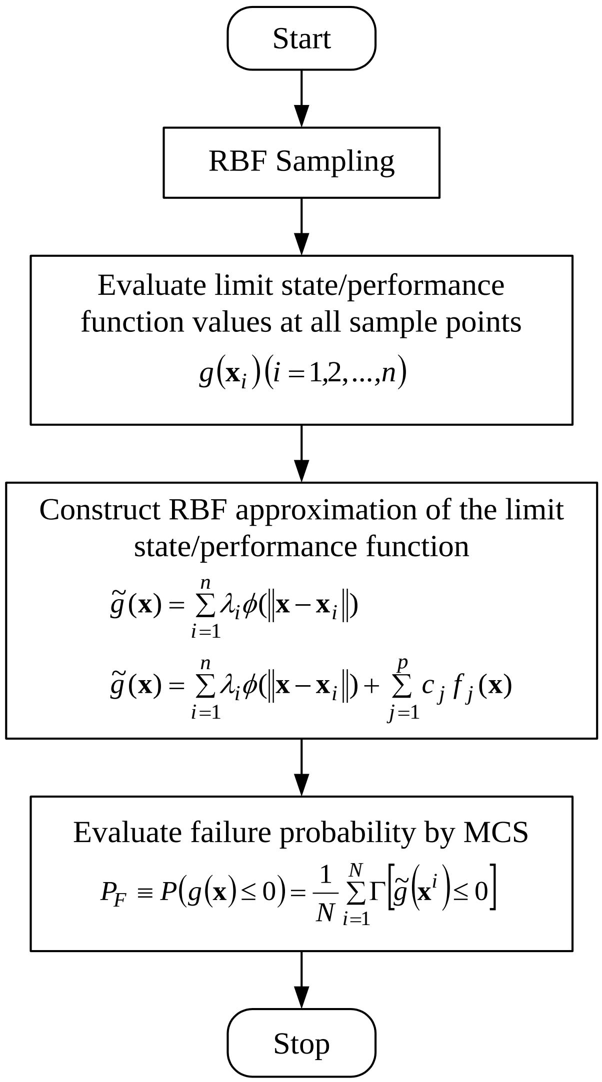

Figure 11. Flow chart of reliability analysis using RBF metamodels [153].

6 APPLICATION TO CONCRETE BARRIERS

6.1 *Background Information*

The proposed reliability analysis approach was applied to the assessment of a concrete barrier, as shown in Figure 6. MASH TL-3 was considered and the performance of the concrete barrier in redirecting a pickup truck was studied. The IM was the impact velocity of the vehicle, and only one velocity value was selected, i.e., impact velocity v = 100 km/h.

6.2 *Random Variables*

In this study, two random variables were considered, i.e., the impact angle and vehicle mass. Table 3 lists the statistical properties of the two variables. Since there are very limited published data in terms of the statistics of impact angle and vehicle mass, an assumption was made that they both followed normal distributions, with their mean values and standard deviations (SDs) listed in Table 3. Note that different types of variable distribution can be considered in the proposed method, once the metamodels are generated. To study the effects of different SDs, three SD values were studied for the vehicle mass, i.e., 100 kg, 150 kg, and 200 kg, although only SD=100 kg is listed in Table 3. The SD value of the impact angle was three degrees, which was considered reasonable based on engineering judgment.

Table 3. Random variables for concrete barriers.

Random variables	Distribution type	Mean	SD
Impact angle (degree)	Normal	25	3
Vehicle mass (kg)	Normal	2638	100

6.3 *Numerical Simulation Matrix and Results*

The simulation matrix of the concrete barrier is shown in Table 4. A 5×7 = 35 simulation matrix was created based on five impact angles (A) and seven vehicle masses (m). The software package HiPPO was used to create the simulation matrix [154]. Thirty-five crash analyses were conducted to obtain the vehicle crash responses. The five impact angles were 19º, 22º, 25º, 28º, and 31º. The vehicle mass included 2,338 kg, 2,438 kg, 2,538 kg, 2,638 kg, 2,738 kg, 2,838 kg, and 2,938 kg. All the values were selected in a range of ±2×SD of the impact angle and ±3×SD of the vehicle mass. The reliability analysis in this example was to evaluate the performance of the concrete barrier with the following scenario: impact velocity v = 100 km/h, impact angle A = 25º, and vehicle mass m = 2,638 kg.

All the numerical simulations were performed using LS-DYNA and the simulation results are listed in Table 5 to Table 15. Table 5 to Table 15 show various crash responses including exit angle, maximum vehicle acceleration, OIV-x, OIV-y, ORA-x, ORA-y, maximum roll and yaw angles, ASI, PHD, and THIV. When different crash responses and corresponding upper limits are considered, the limit state function $g(\mathbf{x})$ in Eq. (5) is written as

$$g(\mathbf{x}) = f^{Limit} - f(\mathbf{x}) \tag{18}$$

where $f(\mathbf{x})$ represents different crash response functions, including those listed in Table 5 to Table 15. f^{Limit} is the upper bound limit of the crash responses considered in the study. The failure of an RSH system is defined as the value of crash response function $f(\mathbf{x})$ exceeding the specified upper bound limit f^{Limit}, i.e., $g(\mathbf{x}) \leq 0$. In this example, the crash failure levels of RSH were determined based on Eq. (18) and the failure probabilities were calculated for various crash responses, when different f^{Limit} bounds were selected.

Table 4. Simulation matrix (5×7 = 35 simulations).

		Impact angle (degree)				
		A=19	A=22	A=25	A=28	A=31
Vehicle mass (kg)	m=2338	√	√	√	√	√
	m=2438	√	√	√	√	√
	m=2538	√	√	√	√	√
	m=2638	√	√	√	√	√
	m=2738	√	√	√	√	√
	m=2838	√	√	√	√	√
	m=2938	√	√	√	√	√

Table 5. Simulation results – Exit angle of vehicle (degree).

		Impact angle (degree)				
		A=19	A=22	A=25	A=28	A=31
Vehicle mass (kg)	m=2338	5.24	5.01	5.69	6.55	5.76
	m=2438	5.38	5.44	5.93	6.86	5.93
	m=2538	5.94	5.24	6.16	6.89	5.94
	m=2638	5.33	5.37	6.38	7.04	5.99
	m=2738	6.07	5.51	6.44	7.11	6.15
	m=2838	6.44	5.79	7.04	6.55	7.36
	m=2938	6.61	6.3	7.14	7.63	6.28

Table 6. Simulation results – Maximum vehicle acceleration (*g*).

		Impact angle (degree)				
		A=19	A=22	A=25	A=28	A=31
Vehicle mass (kg)	m=2338	36.96	38.20	27.31	27.66	27.69
	m=2438	35.80	33.90	27.80	26.83	29.24
	m=2538	34.41	36.49	32.06	29.45	28.30
	m=2638	34.52	35.00	33.89	27.71	28.28
	m=2738	33.53	37.22	31.29	31.38	29.22
	m=2838	35.21	35.61	29.84	31.49	28.51
	m=2938	35.97	37.67	31.12	28.47	30.84

Table 7. Simulation results – OIV-x (*m/s*).

		Impact angle (degree)				
		A=19	A=22	A=25	A=28	A=31
Vehicle mass (kg)	m=2338	4.64	4.72	5.26	4.44	4.47
	m=2438	4.63	4.13	4.02	4.32	3.99
	m=2538	3.83	4.45	4.15	4.47	3.84
	m=2638	4.46	4.30	4.03	4.43	3.80
	m=2738	3.77	4.15	3.99	4.17	3.97
	m=2838	3.77	3.91	4.24	4.17	3.80
	m=2938	3.73	3.90	3.61	3.82	3.67

Table 8. Simulation results – OIV-y (*m/s*).

		Impact angle (degree)				
		A=19	A=22	A=25	A=28	A=31
Vehicle mass (kg)	m=2338	2.73	1.54	1.48	0.89	0.69
	m=2438	2.67	1.34	1.08	0.88	1.50
	m=2538	2.22	1.53	0.91	0.15	1.79
	m=2638	2.70	1.40	0.96	0.31	1.58
	m=2738	2.19	1.42	0.98	0.73	0.89
	m=2838	2.23	1.41	1.40	0.83	0.72
	m=2938	2.32	1.39	1.32	0.64	0.88

Table 9. Simulation results – ORA-x (*g*).

		Impact angle (degree)				
		A=19	A=22	A=25	A=28	A=31
Vehicle mass (kg)	m=2338	2.98	2.57	2.63	2.65	2.07
	m=2438	2.31	3.20	2.75	3.00	2.09
	m=2538	3.44	3.56	3.53	3.41	2.48
	m=2638	2.86	3.16	3.06	4.10	2.51
	m=2738	3.88	3.67	2.79	3.31	2.85
	m=2838	3.58	3.33	2.71	3.41	3.09
	m=2938	3.38	3.32	3.01	2.86	3.12

Table 10. Simulation results – ORA-y (*g*).

	Impact angle (degree)					
		A=19	A=22	A=25	A=28	A=31
Vehicle mass (kg)	m=2338	10.80	12.90	11.11	12.13	11.72
	m=2438	11.31	13.46	13.56	12.44	12.44
	m=2538	11.08	12.13	13.86	11.21	12.84
	m=2638	11.01	11.80	13.75	10.91	12.70
	m=2738	10.80	11.20	13.05	10.40	12.20
	m=2838	9.91	10.60	10.80	10.16	11.11
	m=2938	10.01	9.85	10.50	9.63	10.29

Table 11. Simulation results – Maximum roll angle (degree).

	Impact angle (degree)					
		A=19	A=22	A=25	A=28	A=31
Vehicle mass (kg)	m=2338	29.06	25.87	23.81	21.74	19.50
	m=2438	33.30	27.76	25.34	23.15	21.19
	m=2538	34.21	27.88	27.61	24.32	22.65
	m=2638	36.28	32.76	28.60	25.59	24.40
	m=2738	42.86	35.72	31.79	27.46	25.45
	m=2838	49.15	37.68	29.40	28.73	25.62
	m=2938	56.22	41.61	34.96	29.32	26.53

Table 12. Simulation results – Maximum yaw angle (degree).

	Impact angle (degree)					
		A=19	A=22	A=25	A=28	A=31
Vehicle mass (kg)	m=2338	34.79	35.06	35.30	38.18	40.18
	m=2438	33.44	34.02	35.05	37.45	40.99
	m=2538	31.06	30.84	34.84	37.49	40.37
	m=2638	32.05	34.01	34.86	37.96	39.59
	m=2738	30.35	31.84	33.80	38.44	40.20
	m=2838	30.39	31.23	42.76	38.78	40.73
	m=2938	30.24	31.82	32.80	37.83	40.61

Table 13. Simulation results – ASI.

	Impact angle (degree)					
		A=19	A=22	A=25	A=28	A=31
Vehicle mass (kg)	m=2338	1.52	1.43	1.35	1.29	1.23
	m=2438	1.49	1.43	1.38	1.31	1.23
	m=2538	1.52	1.42	1.35	1.29	1.22
	m=2638	1.47	1.39	1.34	1.32	1.22
	m=2738	1.52	1.41	1.35	1.30	1.21
	m=2838	1.49	1.38	1.38	1.29	1.21
	m=2938	1.48	1.39	1.35	1.27	1.19

Table 14. Simulation results – PHD (*g*).

	Impact angle (degree)					
		A=19	A=22	A=25	A=28	A=31
Vehicle mass (kg)	m=2338	3.27	3.39	3.49	3.44	3.34
	m=2438	3.28	3.45	3.50	3.53	3.40
	m=2538	3.43	3.49	3.54	3.65	3.42
	m=2638	3.34	3.52	3.52	3.60	3.40
	m=2738	3.44	3.54	3.44	3.52	3.36
	m=2838	3.35	3.51	3.51	3.52	3.33
	m=2938	3.31	3.48	3.38	3.43	3.34

Table 15. Simulation results – THIV (*m/s*).

	Impact angle (degree)					
		A=19	A=22	A=25	A=28	A=31
Vehicle mass (kg)	m=2338	9.16	9.21	9.46	9.25	9.20
	m=2438	9.11	9.08	9.33	9.29	9.24
	m=2538	9.12	9.21	9.30	9.34	9.22
	m=2638	9.04	9.45	9.29	9.35	9.15
	m=2738	9.13	9.44	9.26	9.31	9.15
	m=2838	9.10	9.35	9.38	9.28	9.09
	m=2938	9.09	9.31	9.23	9.23	9.08

The crash simulation results at various time steps (0 to 700 *ms*) for m = 2,638 kg and A = 25 degrees are shown in Figure 12. It is seen that in the simulation, the pickup truck was successfully redirected after impacting the concrete barrier.

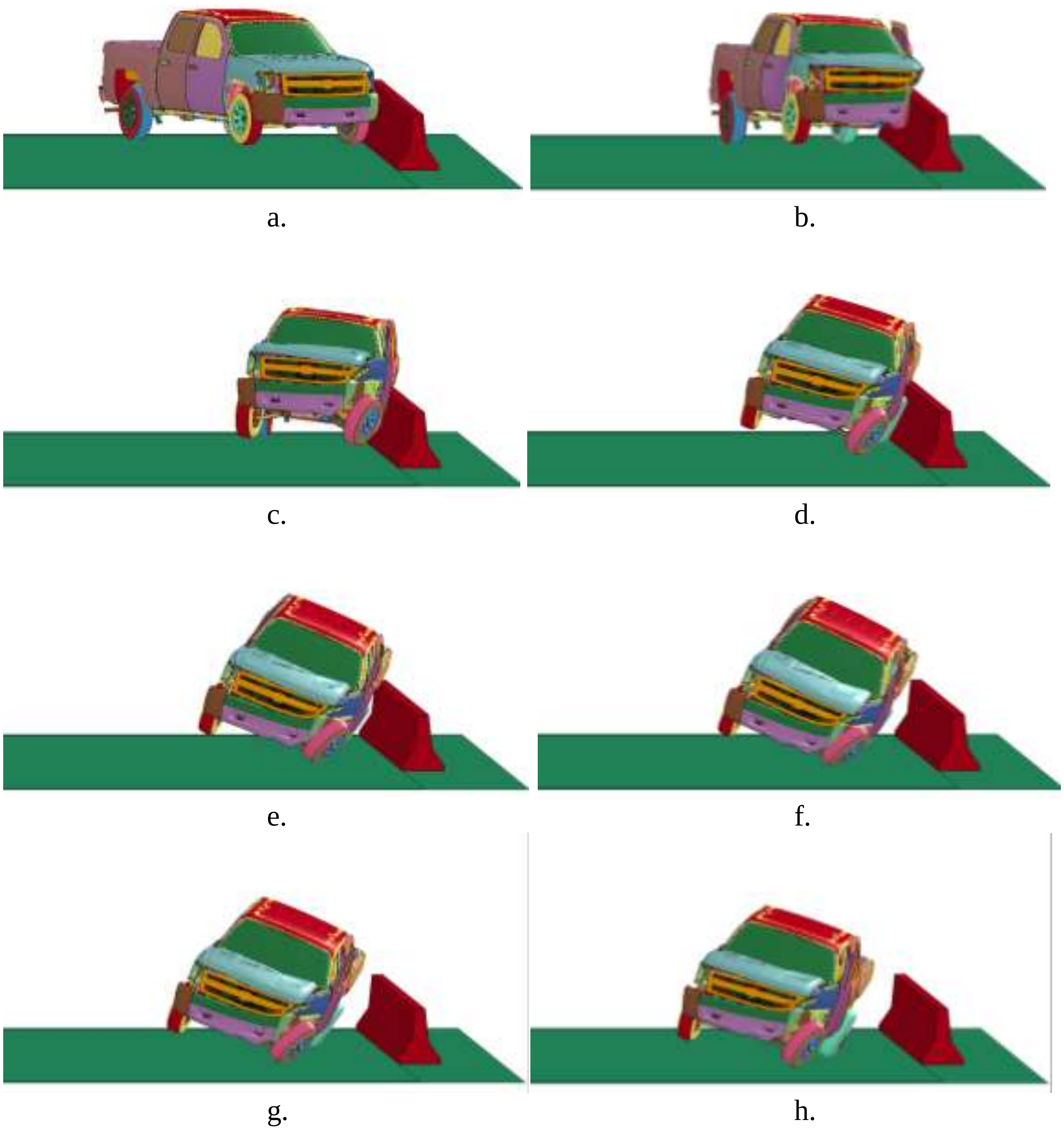

Figure 12. Crash simulation results (m = 2,638 kg, A = 25 degrees).
a.*t = 0 ms*, b. *t = 100 ms*, c. *t = 200 ms*, d. *t = 300 ms*,
e.*t = 400 ms*, f. *t = 500 ms*, g. *t = 600 ms*, and h. *t = 700 ms*.

6.4 *Reliability Analysis Results*

The reliability analysis results are summarized in Figure 13 to Figure 23. Figure 13 to Figure 23 illustrate the failure probability or probability of exceedance (i.e., crash response $f(\mathbf{x})$ exceeds an upper bound limit f^{Limit}) versus the upper bound limit f^{Limit}. The failure probability value varies from 0.0 (no failure) to 1.0 (100% failure). In Figure 13, the crash response is the exit angle of the vehicle after impact. The upper bound limits of exit angle are from 5.5 to 7.5 degrees. As the exit angle limit increases, the probability of failure, P_F, decreases. The three standard derivations produced similar results, as can be seen from Figure 13. The reliability analysis results of the maximum vehicle acceleration (Acc) are shown in Figure 14. The maximum vehicle acceleration limits considered are from 28 *g* to 36 *g*. As the maximum vehicle acceleration limit increases, the probability of failure, P_F, decreases.

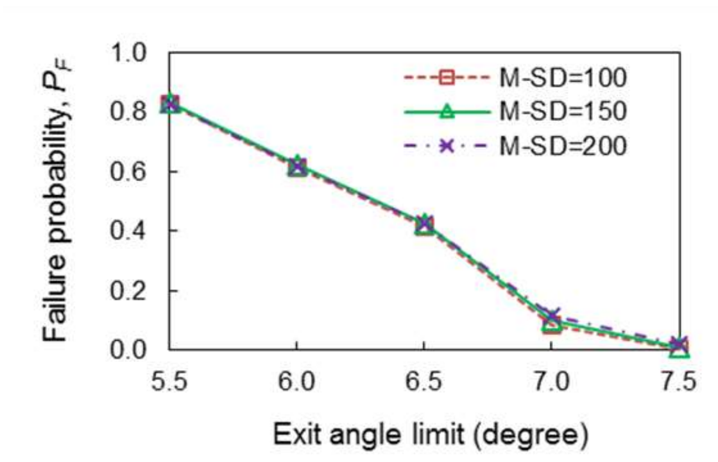

Figure 13. Probability of exceedance vs. exit angle limit.

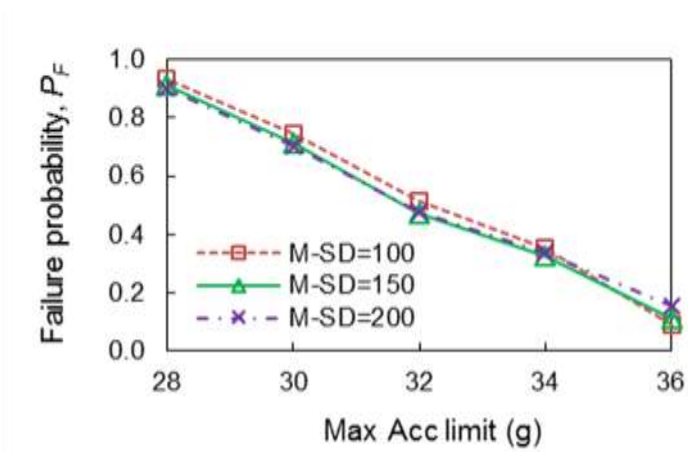

Figure 14. Probability of exceedance vs. maximum vehicle acceleration limit.

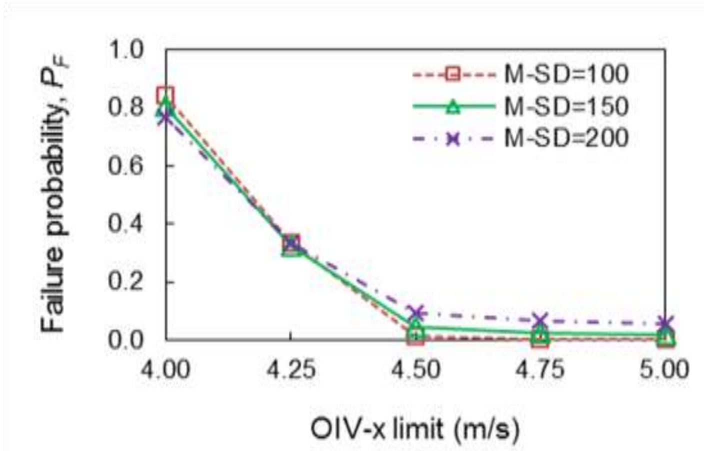

Figure 15. Probability of exceedance vs. OIV-x limit.

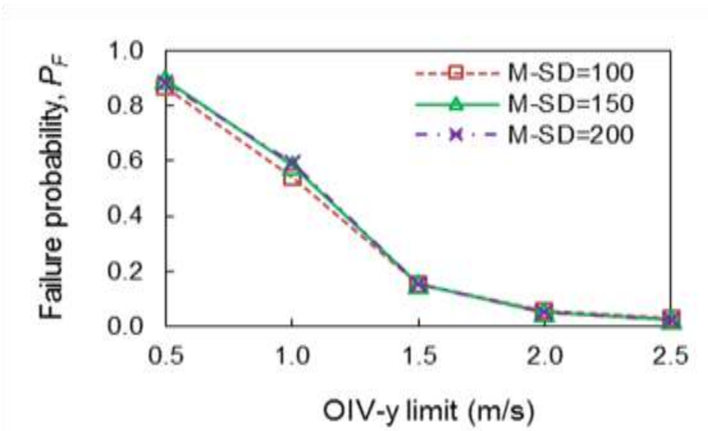

Figure 16. Probability of exceedance vs. OIV-y limit.

The reliability analysis results of OIV-x and OIV-y are shown in Figure 15 and Figure 16, respectively. As expected, as the OIV-x and OIV-y limits increase, the probability of exceedance decreases. The reliability analysis results of the ORA-x and ORA-y are shown in Figure 17 and Figure 18, respectively. As the ORA limits increase, the probability of exceedance decreases.

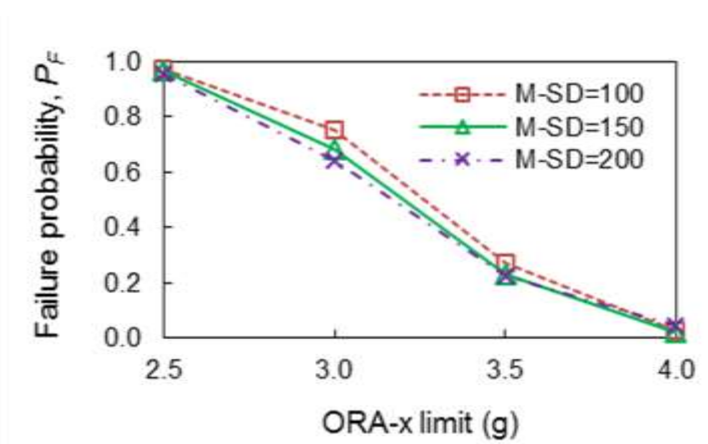

Figure 17. Probability of exceedance vs. ORA-x limit.

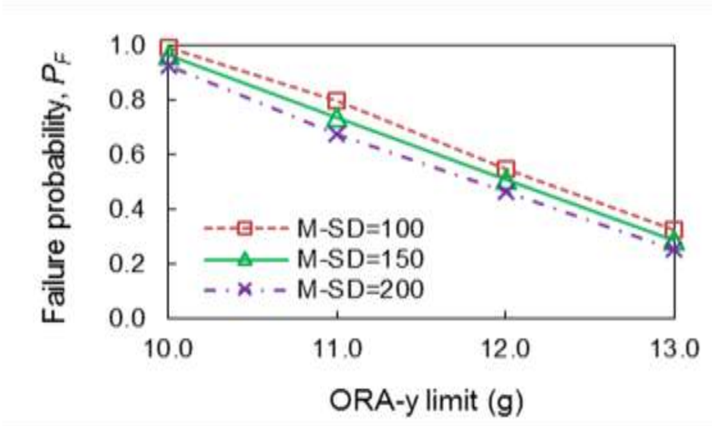

Figure 18. Probability of exceedance vs. ORA-y limit.

The reliability analysis results of maximum vehicle roll angle and yaw angle are shown in Figure 19 and Figure 20, respectively. In the plots, the maximum roll angle limits are from 25º to 45º, and the maximum yaw angle limits are from 32º to 40º. As expected, as the maximum vehicle roll and yaw angle limits increase, the probability of failure, P_F, decreases. The three standard derivations produced similar results, as can be seen from Figure 19 and Figure 20.

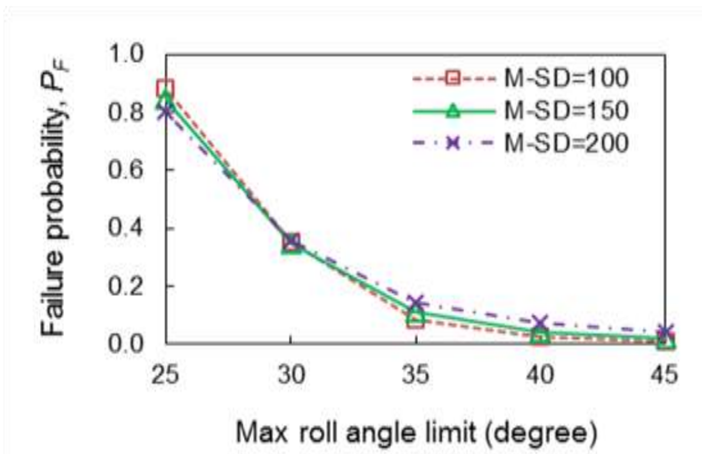

Figure 19. Probability of exceedance vs. maximum vehicle roll angle limit.

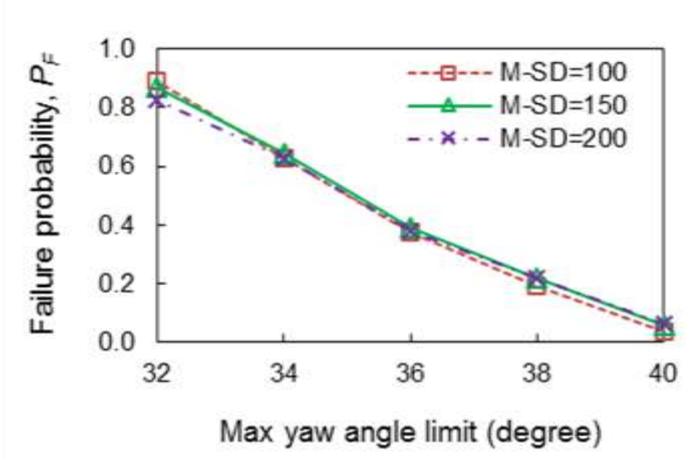

Figure 20. Probability of exceedance vs. maximum vehicle yaw angle limit.

Figure 21, Figure 22, and Figure 23 show the reliability analysis results of ASI, PHD, and THIV, respectively. The ASI limits are from 1.25 to 1.45. As expected, the probability of exceedance decreases as the ASI, PHD, and THIV limit increases, from more than 90% to less than 10% probability of failure, as shown in all three figures.

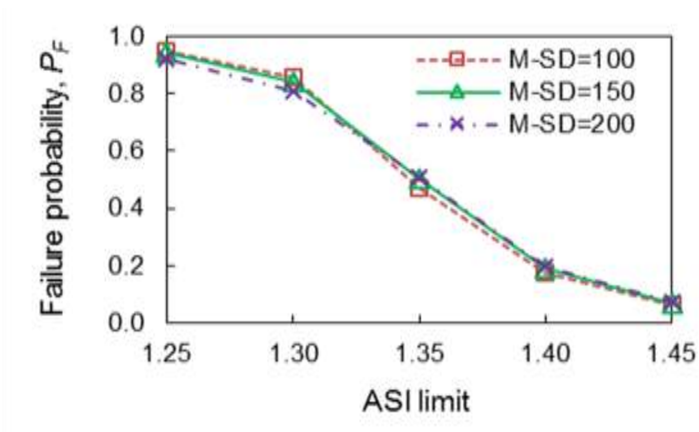

Figure 21. Probability of exceedance vs. ASI limit.

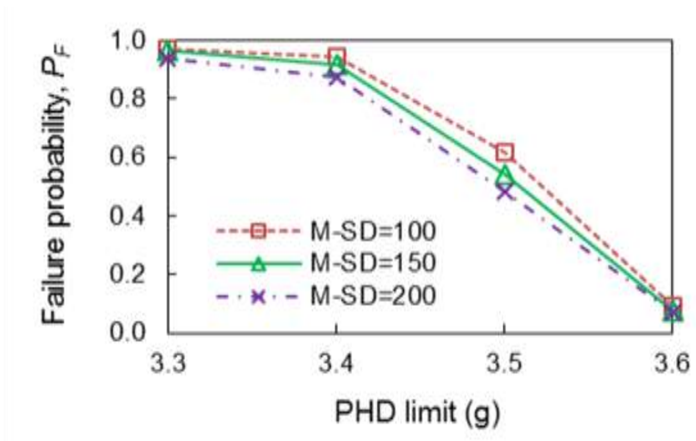

Figure 22. Probability of exceedance vs. PHD limit.

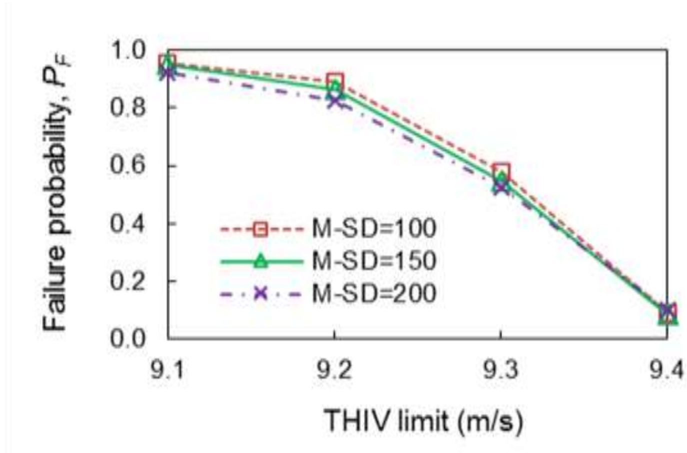

Figure 23. Probability of exceedance vs. THIV limit.

7 SUMMARY AND CONCLUDING REMARKS

To evaluate the performance of RSH and roadway facilities, the failures of RSH systems subjected to vehicle crashes were investigated. A reliability analysis method for assessment of RSH systems was proposed and studied in this project. The reliability analysis method was based on numerical simulations and metamodeling methods at different IMs. In order to reduce computational efforts involved in nonlinear FE analyses, accurate and efficient metamodels using RBFs or augmented RBFs were required. The MCS became straightforward once the explicit metamodels were created. With relatively small sample sizes, the proposed approach worked well. The failure probabilities for all the limit state functions were obtained. In addition, the number of FE analyses, i.e., original limit state function evaluations, was greatly reduced. The proposed approach provides an efficient way to evaluate the reliability of RSH systems, when expensive numerical analyses are required. Although only one metamodel, i.e., RBF-CS20-LP, was used in the current work, a few other RBF metamodels can be applied and produce similar model accuracy.

The proposed reliability analysis approach is general and applicable to various RSH systems under different crash conditions. In this project, a 2007 Chevy Silverado pickup truck impacting a concrete barrier was studied. Nine different crash responses and a total of eleven limit state functions were studied to evaluate the concrete barrier performance in redirecting the vehicle, as well as the occupant responses. The failure probabilities were evaluated according to different limit values of the crash responses. Based on the numerical results, it appeared that the SD value of the vehicle mass did not have a significant impact on the failure probabilities. The reliability analysis results provide useful information of the RSH performance that can be used to improve safety and reduce the costs of RSH systems.

8 FUTURE WORKS

This project provided researchers, owners, and engineers a new probability-based methodology for assessing the performance and failures of RSH systems. More effort is needed to further study the reliability analysis method for design, installation, and retrofit of various RSH systems. Future work is suggested in the following areas:

1. The probability-based method in this project shall be extended to a full vulnerability analysis of RSH systems so that a range of IMs can be considered.

2. In the current project we only focused on concrete barriers. A study of the methodology and its application to other types of RSH systems, such as W-beams and cable barriers, will be beneficial to the transportation community.

3. In this study, only a pickup truck was used for numerical simulations and reliability analyses. However the method can be applied to any other vehicles with different crash conditions. Future work also includes a performance-based method such that multiple vehicles can be considered. This will be of great value to the practicing as well as academic community. In addition, the behaviors of RSH systems impacted by different types of vehicles are different. Vulnerability analysis for RSH subjected to impacts by different types of vehicles shall be performed to give a full spectrum of fragility data in terms of vehicle crashes.

4. Different types of metamodeling methods shall be investigated to maximize the efficiency of the numerical programs. These include kriging, neural networks, HDMR, and other methods.

9 ACKNOWLEDGEMENTS

The research presented in this report was supported by the University Transportation Research Center (UTRC) through Grant # 49198-11-27. The findings reflect the views of the authors who are responsible for the facts and accuracy of the data presented. The contents do not reflect the official views or policies of the Department of Transportation. This report does not constitute a standard, specification, or regulation.

REFERENCES

[1] https://en.wikipedia.org/wiki/File:Concrete-step-barrier-M18.jpg.

[2] http://www.mainlinefence.com/gallery/category/guard-rails.

[3] http://i01.i.aliimg.com/img/pb/933/001/296/296001933_554.jpg.

[4] http://media.mlive.com/kzgazette_impact/photo/9260974-large.jpg.

[5] Committee on Guardrails and Guide Posts (1962). Proposed Full-Scale Testing Procedures for Guardrails. Highway Research Correlation Service Circular 482, Highway Research Board, Washington D.C.

[6] H.E. Ross Jr, D.L. Sicking, R.A. Zimmer, J.D. Michie (1993). Recommended procedures for the safety performance evaluation of highway features. NCHRP Report 350, Transportation Research Board, National Research Council, Washington, D.C.

[7] J.D. Reid, D.L. Sicking, R.K. Faller, B. Pfeifer (1997). Development of a new guardrail system. Transportation Research Record, 1599(1), 72-80.

[8] Plaxico, C.A., Ray, M.H., Hiranmayee, K. (2000). Impact performance of the G4(1W) and G4(2W) guardrail systems: comparison under NCHRP Report 350 test 3-11 conditions. Transportation Research Record, 1720, 7-18.

[9] M. Ray, K. Engstrand, C. Plaxico, R. McGinnis (2001). Improvements to the weak-post W-beam guardrail. Transport Research Record, 1743(1), 88-96.

[10] D.L. Sicking, J.D. Reid, and J.R. Rohde (2002). Development of the midwest guardrail system. Transportation Research Record, 1797, 44-52

[11] G.R. Consolazio, J.H. Chung, K.R. Gurley (2003). Impact simulation and full scale crash testing of a low profile concrete work zone barrier. Computers and Structures, 81, 1359-1374.

[12] R.K. Faller, K.A. Polivka, B.D. Kuipers, R.W. Bielenberg, J.D. Reid, J.R. Rohde, D.L. Sicking (2004). Midwest guardrail system for standard and special applications. Transportation Research Record, 1890(1), 19-33.

[13] A.O. Atahan, Ö. Cansiz (2005). Improvements to G4 (RW) strong-post round-wood, W-beam guardrail system. Journal of Transportation Engineering, 131(1), 63-73.

[14] Z. Ren, M. Vesenjak (2005). Computational and experimental crash analysis of the road safety barrier. Engineering Failure Analysis, 12, 963-973.

[15] Buth CE, Bullard DL, Menges WL (2006). NCHRP Report 350 Test 3-11 of the long-span guardrail with 5.7 m clear span and nested W-beams over 11.4 m. Report 405160-1-1, Texas Transportation Institute, Texas.

[16] C.A. Plaxico, J.C. Kennedy, C.R. Miele CR. (2006). Development of an NCHRP Report 350 TL-3 New Jersey shape 50-inch portable concrete barrier. Final Report FHWA/OH-2006/16, Ohio Department of Transportation.

[17] W.G. Davids, J.K. Botting, M. Peterson (2006). Development and structural testing of a composite-reinforced timber highway guardrail. Construction and Building Materials, 20, 733-743.

[18] R. Faller, D. Sicking, R. Bielenberg, J. Rohde, K. Polivka, J. Reid (2007). Performance of steel-post, W-beam guardrail systems. Transportation Research Record, 2025, 18-33.

[19] R. Faller, J. Reid, D. Kretschmann, J. Hascall, D. Sicking (2009). Midwest Guardrail System with round timber posts. Transportation Research Record, 2120, 47-59.

[20] M. Soltani, T.B. Moghaddam, M.R. Karim, N.H. Sulong (2013). The safety performance of guardrail systems: review and analysis of crash tests data. International Journal of Crashworthiness, 18, 530-543.

[21] AASHTO MASH-1 (2009). Manual for Assessing Safety Hardware (MASH), 1st edition. American association of state highway transportation officials, Washington, D.C.

[22] M.J. Wiebelhaus, R.J. Terpsma, K.A. Lechtenberg, R.K. Faller, D.L. Sicking, R.W. Bielenberg, J.D. Reid, J.R. Rohde (2010). Development of a temporary concrete barrier to permanent concrete median barrier approach transition. Report TRP-03-208-10, Midwest Roadside Safety Facility (MwRSF), Lincoln, NE.

[23] S.K. Rosenbaugh, K.A. Lechtenberg, R.K. Faller, D.L. Sicking, R.W. Bielenberg, J.D. Reid (2010). Development of the MGS approach guardrail transition using standardized steel posts. Report TRP-03-210-10, Midwest Roadside Safety Facility (MwRSF), Lincoln, NE.

[24] M.J. Wiebelhaus, E.A. Johnson, D.L. Sicking, R.K. Faller, K.A. Lechtenberg, J.R. Rohde, R.W. Bielenberg, J.D. Reid, S.K. Rosenbaugh (2011). Phase I Development of a non-proprietary, four-cable, high tension median barrier. Report TRP-03-213-11, Midwest Roadside Safety Facility (MwRSF), Lincoln, NE.

[25] J.D. Schmidt, D.L. Sicking, R.K. Faller, K.A. Lechtenberg, R.W. Bielenberg, J.D. Reid, S.K. Rosenbaugh (2012). Phase II Development of a non-proprietary, four-cable, high tension median barrier. Report TRP-03-253-12, Midwest Roadside Safety Facility (MwRSF), Lincoln, NE.

[26] C.J. Stolle, K.A. Lechtenberg, J.D. Reid, R.K. Faller, R.W. Bielenberg, S.K. Rosenbaugh, D.L. Sicking, E.A. Johnson (2012). Determination of the maximum MGS mounting height – Phase I Crash testing. Report TRP-03-255-12, Midwest Roadside Safety Facility (MwRSF), Lincoln, NE.

[27] R.D. Julin, J.D. Reid, R.K. Faller, M. Mongiardini (2012). Determination of the maximum MGS mounting height – Phase II Detailed analysis using LS-DYNA. Report TRP-03-274-12, Midwest Roadside Safety Facility (MwRSF), Lincoln, NE.

[28] D.A. Gutierrez, K.A. Lechtenberg, R.W. Bielenberg, R.K. Faller, J.D. Reid, D.L. Sicking (2013). Midwest guardrail system (MGS) with southern yellow pine posts. Report TRP-03-272-13, Midwest Roadside Safety Facility (MwRSF), Lincoln, NE.

[29] W.F. Williams, WL. Menges (2011). MASH Test 3-11 of the TxDOT portable Type 2 PCTB with sign support assembly. Report FHWA/TX-11/0-6143-1, Texas Transportation Institute, College Station, Texas.

[30] R.P. Bligh, D.R. Arrington, N.M. Sheikh, C. Silvestri, W.L. Menges (2011). Development of a MASH TL-3 median barrier gate. Report FHWA/TX-11/9-1002-2, Texas Transportation Institute, College Station, Texas.

[31] W.F. Williams, R.P. Bligh, W.L. Menges (2011). MASH Test 3-11 of the TxDOT single slope bridge rail (Type SSTR) on pan-formed bridge deck. Report FHWA/TX-11/9-1002-3, Texas Transportation Institute, College Station, Texas.

[32] R.P. Bligh, A.Y. Abu-Odeh, W.L. Menges (2011). MASH Test 3-10 on 31-inch W-beam guardrail with standard offset blocks. Report FHWA/TX-11/9-1002-4, Texas Transportation Institute, College Station, Texas.

[33] D.R. Arrington, R.P. Bligh, W.L. Menges (2011). MASH Test 3-37 OF the TxDOT 31-inch W-beam downstream anchor terminal. Report FHWA/TX-12/9-1002-6, Texas Transportation Institute, College Station, Texas.

[34] N.M. Sheikh, R.P. Bligh, W.L. Menges (2011). Determination of minimum height and lateral design load for MASH Test Level 4 bridge rails. Report FHWA/TX-12/9-1002-5, Texas Transportation Institute, College Station, Texas.

[35] K. Sennah, B. Juette, A. Weber, C. Witt (2011). Vehicle crash testing on a GFRP-reinforced PL-3 concrete bridge barrier. The 2011 Conference & Exhibition of the Transportation Association of Canada, Edmonton, Canada, Sept. 11-14.

[36] K. Sennah, H.R. Khederzadeh (2012). Development of cost-effective PL-3 concrete bridge barrier reinforced with sand-coated glass fiber reinforced polymer (GFRP) bars: vehicle crash test. Canadian Journal of Civil Engineering, 41(4), 357-367.

[37] C.E. Hampton, H.C. Gabler (2013). Development of a Missing Post Repair Guideline for Longitudinal Barrier Crash Safety. Journal of Transportation Engineering, 139(6), 549-555.

[38] A.O. Atahan, A.Ö. Yücel, M.M. Erdem (2014). Crash testing and evaluation of a new generation L1 containment level guardrail. Engineering Failure Analysis, 38, 25-37.

[39] LSTC (2007). LS-DYNA Keyword User's Manual, Version 971. Livemore Software Technology Corporation, Livermore, CA.

[40] M.H. Ray (1996). Repeatability of full-scale crash tests and criteria for validating simulation results. Transportation Research Record, 1528, 155-160.

[41] M.H. Ray (1996). Use of finite element analysis in roadside hardware design. Transportation Research Circular, 453, 61-71.

[42] M.H. Ray, G.S. Patzner (1997). Finite element model of modified eccentric loader terminal (MELT). Transportation Research Record, 1599, 11-21.

[43] C.A. Plaxico, G.S. Patzner, M.H. Ray (1998). Finite element modeling of guardrail timber posts and the post-soil interaction. Transportation Research Record, 1647, 139-146.

[44] J.D. Reid (1996). Towards the understanding of material property influence on automotive crash structures. Thin-Walled Structures, 24, 285-313.

[45] J.D. Reid (1998). Admissible modeling errors or modeling simplifications. Finite Elements in Analysis and Design, 29, 49-63.

[46] J.D. Reid, B.W. Bielenberg (1999). Using LS-DYNA simulation to solve a design problem: bullnose guardrail example. Transportation Research Record, 1690, 95-102.

[47] A.K. Zaouk, D. Marzougui, N.E. Bedewi (2000). Development of a detailed vehicle finite element model, Part I: methodology. International Journal of Crashworthiness, 5(1), 25-36.

[48] A.K. Zaouk, D. Marzougui, C.D. Kan (2000). Development of a detailed vehicle finite element model, Part II: material characterization and component testing. International Journal of Crashworthiness, 5(1), 37-50.

[49] A.K. Zaouk, N.E. Bedewi, C.D. Kan, D. Marzouigui (1997). Development and evaluation of a C-1500 pickup truck model for roadside hardware impact simulation. Report FHWA-RD-96-212, Federal Highway Administration, Washington, D.C.

[50] P. Tiso, C. Plaxico, M. Ray (2002). Improved truck model for roadside safety simulations: Part II - suspension modeling. Transportation Research Record, 1797, 63-71.

[51] J.D. Reid, D. Marzougui (2002). Improved truck model for roadside safety simulations: Part I - structural modeling. Transportation Research Record, 1797, 53-62.

[52] D. Marzougui, M. Zink, A.K. Zaouk, C.D. Kan, N.E. Bedewi (2004). Development and validation of a vehicle suspension finite element model for use in crash simulations. International Journal of Crashworthiness, 9(6), 565-576.

[53] P. Mohan, D. Marzougui, C-D. Kan (2007). Validation of a single unit truck model for roadside hardware impact. International Journal of Vehicle Systems Modelling and Testing, 2(1), 1-15.

[54] P. Mohan, D. Marzougui, L. Meczkowski, N. Bedewi (2005). Finite element modeling and validation of a 3-strand cable guardrail system. International Journal of Crashworthiness, 10, 267-273.

[55] C.A. Plaxico, J.C. Kennedy, C.R. Miele (2006). Development of an NCHRP Report 350 TL-3 New Jersey shape 50-inch portable concrete barrier. Final Report, Ohio Department of Transportation.

[56] C.A. Plaxico, R.M. Hackett, W. Uddin (1997). Simulation of a vehicle impacting a modified thrie-beam guardrail. Transportation Research Record, 1599, 1-10.

[57] D. Marzougui, G. Bahouth, A. Eskandarian, L. Meczkowski, H. Taylor (2000). Evaluation of portable concrete barriers using finite element simulation. Transportation Research Record, 1720, 1-6.

[58] C.D. Kan, D. Marzougui, G.T. Bahouth, N.E. Bedewi (2001). Crashworthiness evaluation using integrated vehicle and occupant finite element models. International Journal of Crashworthiness, 6, 387-398.

[59] A.O. Atahan (2002). Finite element simulation of a strong-post W-beam guardrail system. Simulation, 78(10), 587-599.

[60] C.A. Plaxico, F. Mozzarelli, M.H. Ray (2003). Tests and simulation of a w-beam rail-to-post connection. International Journal of Crashworthiness, 8(6), 543-551.

[61] J. Mackerle (2003). Finite element crash simulations and impact-induced injuries: an addendum. A bibliography (1998–2002). The Shock and Vibration Digest, 35(4), 273-280.

[62] A.O. Atahan (2003). Impact behaviour of G2 steel weak-post W-beam guardrail on nonlevel terrain. International Journal of Heavy Vehicle Systems, 10(3), 209-223.

[63] F. Orengo, M.H. Ray, C.A. Plaxico (2003). Modeling tire blow-out in roadside hardware simulations using LS-DYNA. IMECE2003-55057, The 2003 ASME International Mechanical Engineering Congress & Exposition, Washington, D.C.

[64] R.P. Bligh, A.Y. Abu-Odeh, M.E. Hamilton, N.R. Seckinger (2004). Evaluation of roadside safety devices using finite element analysis. Report FHWA/TX-04/0-1816-1, Texas Transportation Institute, College Station, TX.

[65] M.H. Ray, E. Oldani, C.A. Plaxico (2004). Design and analysis of an aluminum F-shape bridge railing. International Journal of Crashworthiness, 9(4), 349-363.

[66] J.D. Reid (2004). LS-DYNA simulation influence on roadside hardware. Transportation Research Record, 1890, 34-41.

[67] J.D. Reid, B.A. Coon, B.A. Lewis, S.H. Sutherland, Y.D. Murray (2004). Evaluation of LS-DYNA soil material model 147. FHWA-HRT-04-094, U.S. Department of Transportation, Federal Highway Administration, McLean, VA.

[68] J.D. Reid, N.R. Hiser (2004). Friction modelling between solid elements. International Journal of Crashworthiness, 9(1), 65-72.

[69] H.A. Whitworth, R. Bendidi, D. Marzougui, R. Reiss (2004). Finite element modeling of the crash performance of roadside barriers. International Journal of Crashworthiness, 9(1), 35-43.

[70] J.D. Reid, N.R. Hiser (2005). Detailed modeling of bolted joints with slippage. Finite Elements in Analysis and Design, 41, 547-562.

[71] A.O. Atahan, O.F. Cansiz (2005). Crashworthiness analysis of a bridge rail-to-guardrail transition. Finite Elements in Analysis and Design, 41, 371-396.

[72] O.F. Cansiz, A.O. Atahan (2006). Crash test simulation of a modified thrie-beam high containment level guardrail under NCHRP Report 350 TL 4-12 conditions. International Journal of Heavy Vehicle Systems, 13, 2-18.

[73] M. Borovinsek, M. Vesenjak, M. Ulbin, Z. Ren (2007). Simulation of crash tests for high containment levels of road safety barriers. Engineering Failure Analysis, 14, 1711-1718.

[74] P. Mohan, D. Marzougui, C.D. Kan (2007). Validation of a single unit truck model for roadside hardware impact. International Journal of Vehicle Systems Modelling and Testing, 2(1), 1-15.

[75] D. Marzougui, P. Mohan, C.D. Kan, K.S. Opiela (2007). Evaluation of rail height effects on the safety performance of W-beam barriers. 2007 TRB Annual Meeting, Washington, D.C.

[76] J.D. Reid, B.D. Kuipers, D.L. Sicking, R.K. Faller (2009). Impact performance of W-beam guardrail installed at various flare rates. International Journal of Impact Engineering, 36, 476-485.

[77] D. Marzougui, U. Mahadevaiah, C.D. Kan, K. Opiela (2009). Analyzing the effects of cable barriers behind curbs using computer simulation. NCAC 2009-W-008, The National Crash Analysis Center, George Washington University, Washington, D.C.

[78] M.R. Ferdous, A. Abu-Odeh, R.P. Bligh, H.L. Jones, N.M. Sheikh (2011). Performance limit analysis for common roadside and median barriers using LS-DYNA. International Journal of Crashworthiness, 16(6), 691-706.

[79] Ali Osman Atahan, Turan Arslan. (2012) Collision behaviour of double W-beam transition. International Journal of Heavy Vehicle Systems, 19(1), 76-91.

[80] D. Marzougui, P. Mohan, C.D. Kan, K.S. Opiela (2012). Assessing options for improving barrier crashworthiness using finite element models and crash simulations. Final Report NCAC-2012-W-008, National Crash Analysis Center, George Washington University, Washington, D.C.

[81] D. Marzougui, C.D. Kan, K.S. Opiela (2012). Comparison of crash test and simulation results for impact of silverado pickup into New Jersey barrier under Manual for Assessing Safety Hardware. Transportation Research Record, 2309, 114-126.

[82] D. Marzougui, C.D. Kan, K.S. Opiela (2013). Crash test & simulation comparisons of a pickup truck & a small car oblique impacts into a concrete barrier. The 13th International LS-DYNA Users Conference, Dearborn, MI.

[83] Q. Wang, H. Fang, N. Li, D.C. Weggel, G. Wen (2013). An efficient FE model of slender members for crash analysis of cable barriers. Engineering Structures, 52, 240-256.

[84] H. Fang, Q. Wang, D.C. Weggel (2015). Crash analysis and evaluation of cable median barriers on sloped medians using an efficient finite element mode. Advances in Engineering Software, 82, 1-13.

[85] Li, N., Fang, H., Zhang, C., Gutowski, M., Palta, E., and Wang, Q. (2015). A numerical study of occupant responses and injuries in vehicular crashes into roadside barriers based on finite element simulations. Advances in Engineering Software, 90, 22-40.

[86] H. Fang, M. Rais-Rohani, Z. Liu, M.F. Horstemeyer (2005). A comparative study of metamodeling methods for multi-objective crashworthiness optimization. Computers & Structures, 83, 2121-2136.

[87] Y. Xiang, Q. Wang, Z. Fan, H. Fang (2006). Optimal crashworthiness design of a spot-welded thin-walled hat section, Finite Elements in Analysis and Design, 42(10), 846-855.

[88] S. Hou, Q. Li, S. Long, X. Yang, W. Li (2007). Design optimization of regular hexagonal thin-walled columns with crashworthiness criteria. Finite Elements in Analysis and Design, 43, 555-565.

[89] S. Hou, Q. Li, S. Long, X. Yang, W. Li (2008). Multiobjective optimization of multi-cell sections for the crashworthiness design. International Journal Impact Engineering, 2008, 35(11), 1355-1367.

[90] X. Liao, Q. Li, X. Yang, W. Zhang, W. Li (2008) Multiobjective optimization for crash safety design of vehicles using stepwise regression model. Structural & Multidisciplinary Optimization, 35(6), 561-569.

[91] M.F. Horstemeyer, X. Ren, H. Fang, E. Acar, P.T. Wang (2009). A comparative study of design optimization methodologies for side-impact crashworthiness using injury-based versus energy-based criterion, International Journal of Crashworthiness, 14(2), 125-138.

[92] S. Hou, Q. Li, S. Long, X. Yang, W. Li (2009). Crashworthiness design for foam filled thin-walled structures. Materials & Design, 30(6), 2024-2032.

[93] J. Bi, H. Fang, Q. Wang, X. Ren (2010). Modeling and optimization of foam-filled thin-walled columns for crashworthiness designs, Finite Elements in Analysis and Design, 46(9), 698-709.

[94] H. Yin, G. Wen, S. Hou, K. Chen (2011). Crushing analysis and multiobjective crashworthiness optimization of honeycomb-filled single and bitubular polygonal tubes. Materials & Design, 32, 4449-4460.

[95] Hou SJ, Liu TY, Dong D, Han X. (2014). Factor screening and multivariable crashworthiness optimization for vehicle side impact by factorial design. Structural & Multidisciplinary Optimization, 49, 147-167.

[96] S. Hou, Y. Zheng, J. Xie, X. Han X (2014). Optimization design of NJ shaped guardrail based on collision safety consideration, International Journal of Computational Methods, 11, 1350083-1-20.

[97] S. Hou, W. Tan, Y. Zheng, X. Han, Q. Li (2014). Optimization design of corrugated beam guardrail based on RBF-MQ surrogate model and collision safety consideration. Advances in Engineering Software, 78, 28-40.

[98] Yin, H., Fang, H., Wang, Q., and Wen, G. (2016). Design optimization of a MASH TL-3 concrete barrier using RBF based metamodels and nonlinear finite element simulations. Engineering Structures, 114, 122-134.

[99] Rubinstein, R.Y. (1981). Simulation and the Monte Carlo Method. Wiley: New York, NY.

[100] Melchers, R.E. (1999). Structural Reliability Analysis and Prediction. Wiley: Chichester.

[101] Lee, T.-H. and Mosalam, K.M. (2005). Seismic demand sensitivity of reinforced concrete shear-wall building using FOSM method. Earthquake Engineering and Structural Dynamics. 34(14), 1719-1736.

[102] Floren, A. and Mohammadi, J. (2001). Performance-based design approach in seismic analysis of bridges. Journal of Bridge Engineering, 6(1), 37-45.

[103] Filiatrault, A. and Folz, B. (2002). Performance-based seismic design of wood framed buildings. Journal of Structural Engineering, ASCE, 128(1), 39-47.

[104] Zou, X.-K., Chan, C.-M., Li, G. and Wang, Q. (2007). Multi-objective optimization for performance-based design of reinforced concrete frames. Journal of Structural Engineering, ASCE, 133(10), 1462-1474.

[105] Liew, J.Y.R., Tang, L.K. and Choo, Y.S. (2002). Advanced analysis for performance-based design of steel structures exposed to fires. Journal of Structural Engineering, ASCE, 128(12), 1584-1593.

[106] Ciampoli, M., Petrini, F. and Augusti, G. (2009). A procedure for performance-based wind engineering. Proceedings, International Conference on Structural Safety and Reliability, Osaka, Japan; September 13-17.

[107] Foley, C.M., Pezeshk, S. and Alimoradi, A. (2007). Probabilistic performance-based optimal design of steel moment-resisting frames. I: formulation. Journal of Structural Engineering, ASCE, 133(6), 757-766.

[108] Zou, X.-K., Wang, Q., Li, G. and Chan, C.-M. (2010). Integrated reliability-based seismic drift design optimization of base-isolated concrete buildings. Journal of Structural Engineering, ASCE, 136(10), 1282-1295.

[109] Erberik, M.A. and Elnashai, A.S. (2004). Fragility analysis of flat-slab structures. Engineering Structures, 26(7), 937-948.

[110] Kim, J.H. and Rosowsky, D.V. (2005). Fragility analysis for performance-based seismic design of engineered wood shearwalls. Journal of Structural Engineering, ASCE, 131(11), 1764-1773.

[111] Lupoi G., Franchin P., Lupoi A. and Pinto P. (2006). Seismic fragility analysis of structural systems. Journal of Engineering Mechanics, ASCE, 132(4), 385-95.

[112] Padgett, J.E. and DesRoches, R. (2008). Methodology for the development of analytical fragility curves for retrofitted bridges. Earthquake Engineering and Structural Dynamics, 37(8), 1157-1174.

[113] Ji, J., Elnashai, A.S. and Kuchma, D.A. (2007). An analytical framework for seismic fragility analysis of RC high-rise buildings. Engineering Structures, 29(12), 3197-3209.

[114] Seyedi1, D.M., Gehl, P. Douglas, J., Davenne, L., Mezher, N. and Ghavamian, S. (2010). Development of seismic fragility surfaces for reinforced concrete buildings by means of nonlinear time-history analysis. Earthquake Engineering and Structural Dynamics, 39(1), 91-108.

[115] Faravelli L. (1989). Response surface approach for reliability analysis. Journal of Engineering Mechanics, ASCE, 115(12), 2763-2781.

[116] Rajashekhar MR, Ellingwood BR. (1993). A new look at the response surface approach for reliability analysis. Structural Safety, 12(3), 205-220.

[117] Kim SH, Na SW. (1997). Response surface method using vector projected sampling points. Structural Safety, 19(1), 3-19.

[118] Gayton N, Bourinet JM, Lemaire M. (2003). CQ2RS: A new statistical approach to the response surface method for reliability analysis. Structural Safety, 25(1), 99-121.

[119] Zheng Y, Das PK. (2000). Improved response surface method and its application to stiffened plate reliability analysis. Engineering Structures, 22(5), 544-551.

[120] Gavin HP, Yau SC. (2008). High-order limit state functions in the response surface method for structural reliability analysis. Structural Safety, 30(2), 162-179.

[121] Kang S-C, Koh H-M, Choo JF. (2010). An efficient response surface method using moving least square approximation for structural reliability analysis. Probabilistic Engineering Mechanics, 25, 365-371.

[122] Xiang Y, Wang Q, Fan Z, Fang H. (2006). Optimal crashworthiness design of a spot-welded thin-walled hat section. Finite Elements in Analysis and Design, 42(10), 846-855.

[123] Hou S, Li Q, Long S, Yang X, Li W. (2007). Design optimization of regular hexagonal thin-walled columns with crashworthiness criteria. Finite Elements in Analysis and Design, 43, 555-565.

[124] Bi J, Fang H, Wang Q, Ren X. (2010). Modeling and optimization of foam-filled thin-walled columns for crashworthiness designs. Finite Elements in Analysis and Design, 46(9), 698-709.

[125] Youn BD, Choi KK. (2004). A new response surface methodology for reliability-based design optimization. Computers & Structures, 82, 241-256.

[126] Gu X, Sun G, Li G, Mao L, Li Q. (2013). A comparative study on multiobjective reliable and robust optimization for crashworthiness design of vehicle structure. Structural and Multidisciplinary Optimization, 48, 669-684.

[127] Jin R, Chen W, Simpson TW. (2001). Comparative studies of metamodeling techniques under multiple modeling criteria. Structural and Multidisciplinary Optimization, 23, 1-13.

[128] Simpson TW, Mauery TM, Korte JJ, Mistree F. (2001). Kriging metamodels for global approximation in simulation-based multidisciplinary design optimization. AIAA Journal, 39(12), 2233-2241.

[129] Gomes HM, Awruch AM. (2004). Comparison of response surface and neural network with other methods for structural reliability analysis. Structural Safety, 26, 49–67.

[130] Dai HZ, Zhao W, Wang W, Cao ZG. (2011). An improved radial basis function network for structural reliability analysis. Journal of Mechanical Science and Technology, 25(9), 2151-2159.

[131] Chowdhury R, Rao BN, Prasad AM. (2009). High-dimensional model representation for structural reliability analysis. Communications in Numerical Methods in Engineering, 25, 301-337.

[132] Chowdhury R, Rao BN. (2009). Assessment of high dimensional model representation techniques for reliability analysis. Probabilistic Engineering Mechanics, 24, 100-115.

[133] Rao BN, Chowdhury R. (2009). Enhanced high-dimensional model representation for reliability analysis. International Journal for Numerical Methods in Engineering, 77, 719-750.

[134] Bucher C, Most T. A comparison of approximate response functions in structural reliability analysis. Probabilistic Engineering Mechanics 2008; 23:154-163.

[135] Bai YC, Han X, Jiang C, Liu J. (2012). Comparative study of metamodeling techniques for reliability analysis using evidence theory. Advances in Engineering Software, 53, 61-71.

[136] Hardy RL. (1971). Multiquadratic equations of topography and other irregular surfaces. Journal of Geophysical Research, 76(8), 1905-1915.

[137] Krishnamurthy T. (2003). Response surface approximation with augmented and compactly supported radial basis functions. Technical Report AIAA-2003-1748, AIAA.

[138] Fang, H, Rais-Rohani, M, Liu Z, Horstemeyer, MF. (2005). A comparative study of metamodeling methods for multi-objective crashworthiness optimization. Computers & Structures, 83(25-26), 2121-2136.

[139] Fang, H., Horstemeyer MF. (2006). Global response approximation with radial basis functions. Engineering Optimization, 38(04), 407-424.

[140] Fang H, Wang Q. (2008). On the effectiveness of assessing model accuracy at design points for radial basis functions. Communications in Numerical Methods in Engineering, 24(3), 219-235.

[141] Wu, Z. (1995). Compactly supported positive definite radial function. Advances in Computational Mathematics, 4, 283-292.

[142] Council, F.M., Stewart, J.R. (1993). Attempt to Define Relationship Between Forces to Crash-test Vehicles and Occupant Injury in Similar Real-world Crashes, Transportation Research Record, 78-78.

[143] Michie, J.D. (1981). Collision Risk Assessment Based on Occupant Flail-space Model, Transportation Research Record.

[144] NCAC (2009). Development & initial validation of a 2007 Chevrolet Silverado finite element model. Report NCAC 2009-T-005, National Crash Analysis Center, The George Washington University, Washington D.C.

[145] NCAC (2009). Modeling, testing & validation of the 2007 Chevrolet Silverado finite element model. Report NCAC 2009-W-005, National Crash Analysis Center, The George Washington University, Washington D.C.

[146] NCAC (2009). Component and full-Scale tests of the 2007 Chevrolet Silverado suspension system. Report NCAC 2009-R-004, National Crash Analysis Center, The George Washington University, Washington D.C.

[147] NCAC (2012). Extended Validation of the Finite Element Model for the 2007 Chevrolet Silverado Pick-Up Truck. Report NCAC 2012-W-003, National Crash Analysis Center, The George Washington University, Washington D.C.

[148] Madsen, HO, Krenk, S, Lind, NC. (1986). Methods of Structural Safety. Englewood Cliffs, NJ: Printice-Hall.

[149] Ditlevsen, O, Madsen, HO. (1996). Structural Reliability Methods. Chichester: Wiley.

[150] Kiureghian D, Lin H-Z, Hwang S-J. (1987). Second order reliability approximations. Journal of Engineering Mechanics, ASCE, 113(8), 1208-1225.

[151] Montgomery DC. (2001). Design and Analysis of Experiments. New York: John Wiley & Sons, Inc.

[152] Taguchi G. (1993). Taguchi Method-Design of Experiments, Quality Engineering Series Vol. 4. Tokyo: Japanese Standards Association, ASI Press.

[153] Wang, Q., Fang, H., and Shen, L. (2016). Reliability analysis of tunnels using a meta-modeling technique based on augmented radial basis functions. Tunnelling and Underground Space Technology, 56, 45-53.

[154] Fang H, Horstemeyer MF. (2005). HiPPO: an object-oriented framework for general purpose design optimization. Journal of Aerospace Computing, Information, and Communication, 2(12), 490-506.

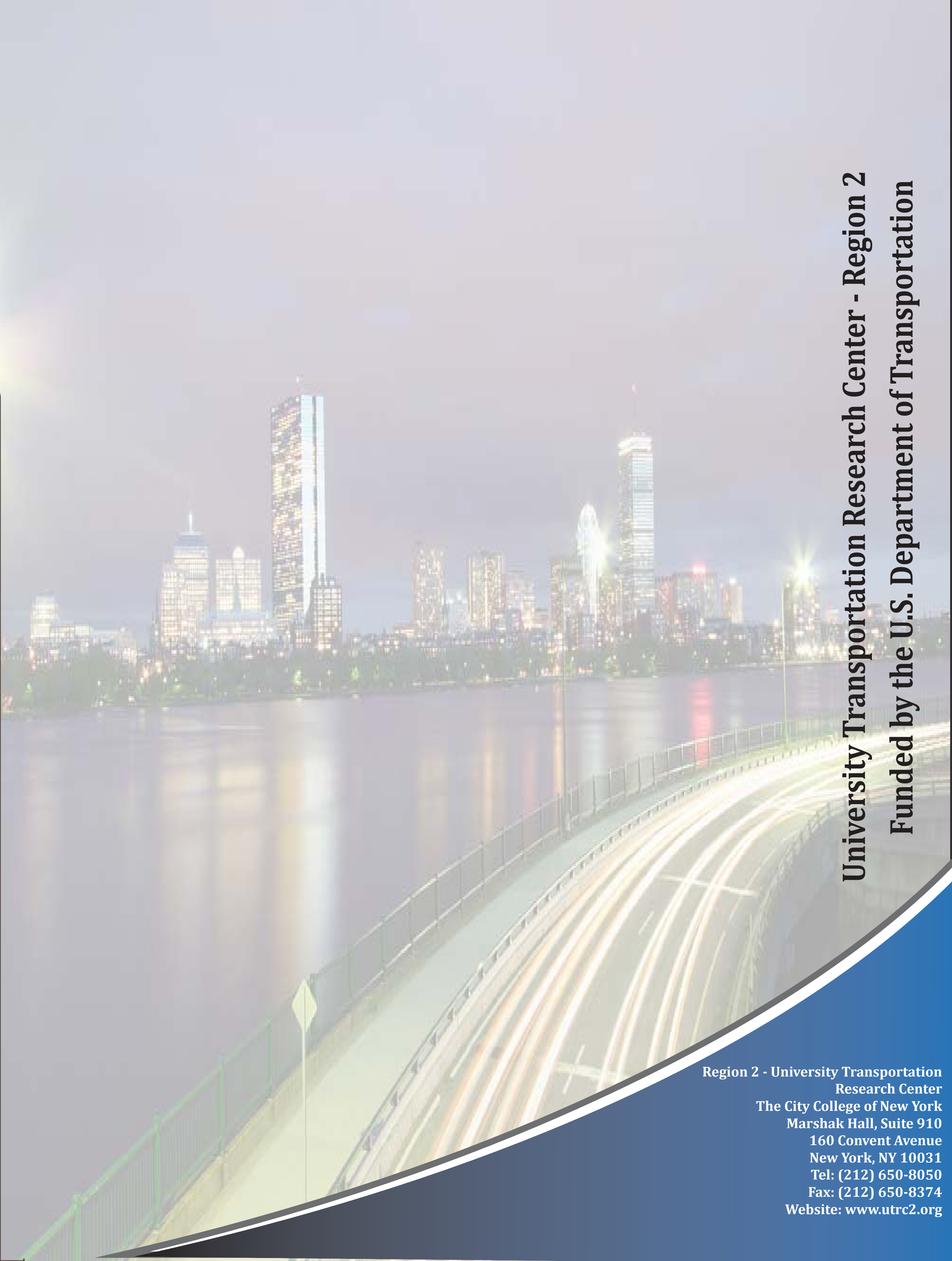

University Transportation Research Center - Region 2
Funded by the U.S. Department of Transportation

Region 2 - University Transportation Research Center
The City College of New York
Marshak Hall, Suite 910
160 Convent Avenue
New York, NY 10031
Tel: (212) 650-8050
Fax: (212) 650-8374
Website: www.utrc2.org